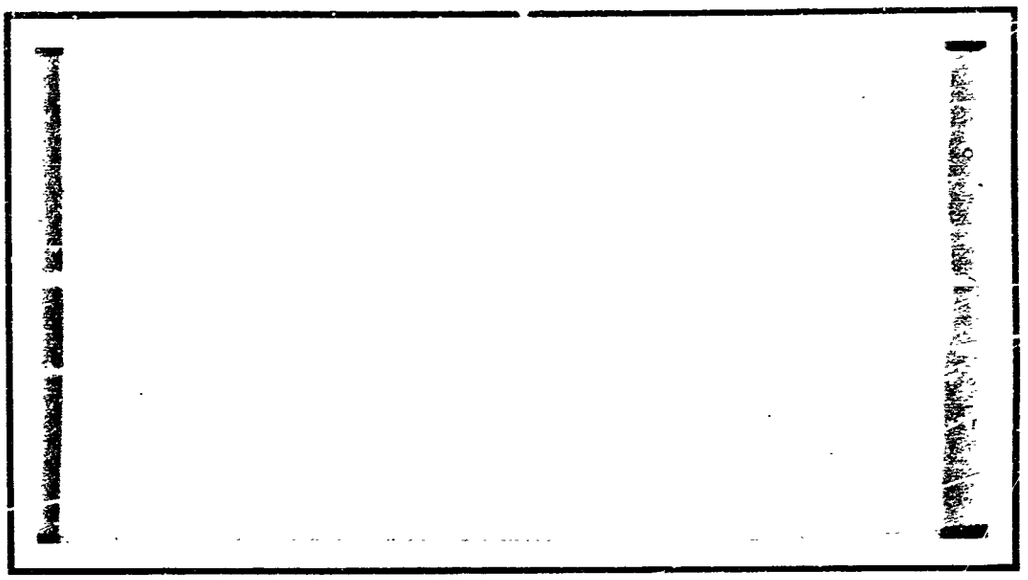

GPO PRICE $ _____

CFSTI PRICE(S) $ _____

Hard copy (HC) 2.50

Microfiche (MF) .75

ff 653 July 65

rantec®

RANTEC CORPORATION
CALABASAS, CALIFORNIA

Rantec No. 31796-FR1 15 June 1966

FINAL ENGINEERING REPORT

CASSEGRAIN ANTENNA FEED SYSTEM

MODEL ASF-108

Prepared for

NATIONAL AERONAUTICS AND SPACE ADMINISTRATION

RANTEC CORPORATION
CALABASAS, CALIFORNIA

TABLE OF CONTENTS

LIST OF ILLUSTRATIONS

LIST OF TABLES

SECTION I

SCOPE OF FINAL REPORT

This final report discusses the Rantec ASF-108 Feed System in terms of the engineering concepts used and design problems encountered during the program. The Cassegrain Feed System is installed on the Rosman 85-foot Antenna No. 2, at Rosman, North Carolina.

The system electrical performance as delineated in the Acceptance Test Report is reviewed and certain aspects of the test report enlarged upon.

This report does not repeat matter contained in References 1 and 2 below but presumes the reader is familiar with the detailed information contained therein.

SECTION II

PURPOSE OF EQUIPMENT

The 85-foot antenna feed will be used for the Advanced Technological Satellite (ATS), which aims to extend the art of space communication through experimentation. Among the experiments will be an investigation of the multiple access concept of communication using phase modulation and an investigation of spacecraft stabilization techniques.

The system is designed for reception in the 4.0 - 4.2 Gc band and transmission in the 6.0 - 6.4 Gc band. While the ASF-108 System is primarily for the ATS mission, it can be used for Comsat and Relay satellites which operate in the same frequency bands.

SECTION III

REFERENCE DOCUMENTS

1. Technical Manual, Cassegrain Antenna Feed System, Model ASF-108. Rantec Pub. No. 31796-TM.

2. Acceptance Test Report, Antenna Feed System, Rantec Model No. ASF-108, Rantec Pub. No. 31796-ATR-1.

3. Performance Specification for a Cassegrain Feed System for 85-foot Antenna, NASA, Goddard Space Flight Center, Spec No. GSFC-TRS-ANT-23, Rev. 1.

4. Functional Specifications for Collimation Tower Equipment, NASA, Goddard Space Flight Center, Spec No. GSFC-TRS-ANT-24, Revision 0.

SECTION IV

SYSTEM CONFIGURATION

A photograph of the feed cone and hyperbolic subreflector installed on the 85-foot parabolic dish is shown in Figure 4-1. The geometry of the Cassegrain System is shown in Figure 4-2. The 11-foot diameter subreflector was selected to adequately cover the 9-foot square quadrapod apex structure and existing 8-foot square low-frequency feed ground plane mounted there without adding additional aperture blocking. The hyperboloid focal length, i.e., the distance between the 85-foot parabola focal point and the feed point, is 22 feet with the feed support cone protruding 14 feet from the parabolic surface.

A block diagram of the equipment configuration is shown in Figure 4-3. The essential features of the system are:

a. Use of a single horn for transmit, receive, and the monopulse sum channel,

b. Use of a circularly polarized ring array for the monopulse error channels,

c. Polarization sensing on the null in the orthogonally polarized receive output using the beacon signal and a dual channel phase lock receiver,

d. Manual polarization rotation over a 270° sector,

e. Inclusion of the Maser in the rotating assembly,

f. Extraction of beacon signal for the monopulse sum channel after amplification by the Maser, and use of a phase compensating rotary joint to maintain relative phase with the circularly polarized error channel array,

g. A Cassegrain subreflector, 11-feet in diameter with a 22-foot focal length. This results in the feed aperture position 14 feet from the 85-foot reflector vertex. The reflector angular full width is 32° 22' at the feed point, and

h. Receive multiplexing after amplification by Maser preamplifier and TWT.

Figure 4-1. ASF-108 Cassegrain Feed System in Rosman 85-foot Antenna No. 2

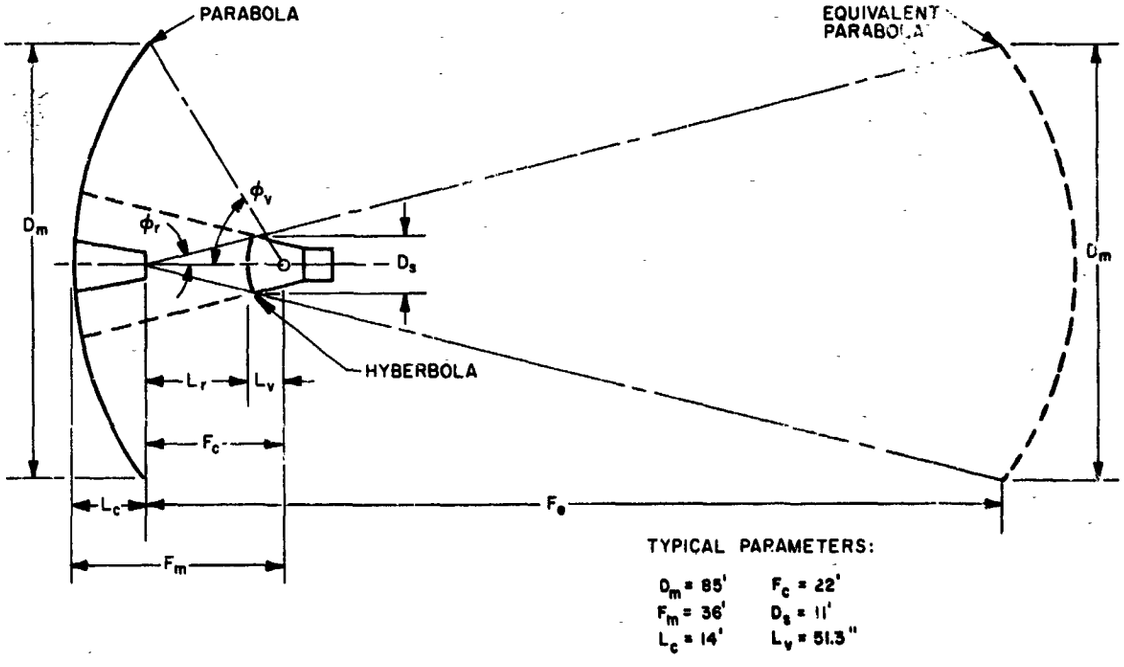

Figure 4-2. Cassegrain Geometry

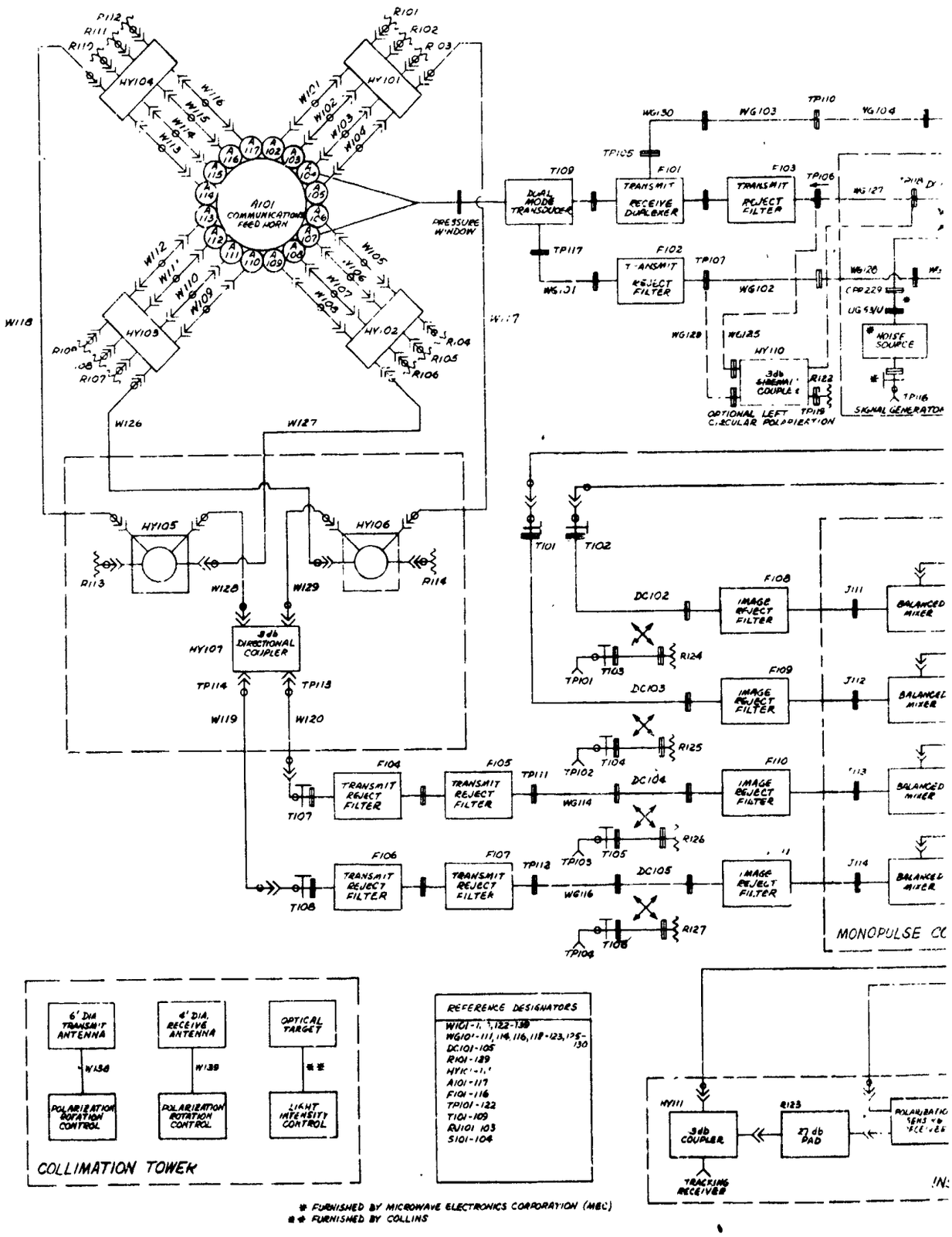

* FURNISHED BY MICROWAVE ELECTRONICS CORPORATION (MEC)
** FURNISHED BY COLLINS

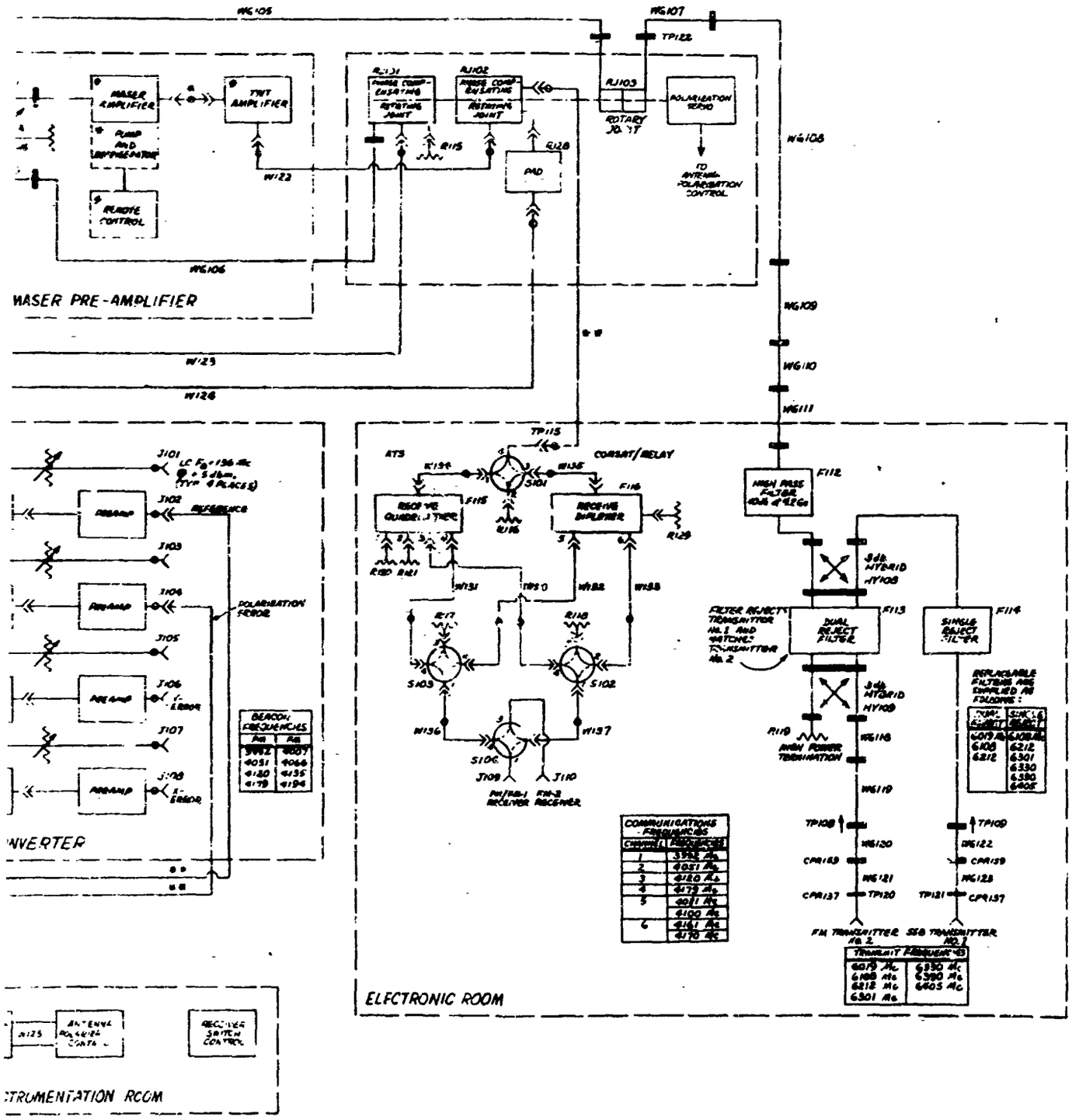

Figure 4-3. Block Diagram, Cassegrain Feed System, Model ASF-108

2

A101	31796117	Communication Unit
2	335-1	Frame Assy
3	409-1	"
4	409-2	"
5	335-2	"
6	335-1	"
7	409-1	"
8	409-2	"
9	335-2	"
10	335-1	"
11	409-1	"
12	409-2	"
13	335-2	"
14	335-1	"
15	409-1	"
16	409-2	"
17	335-2	"

DC101	31796455	26 db Coupler
2	429	Directional Coupler
3	423	"
4	441-2	"
5	441-1	"

F101	31796333	Transmit Receiver Duplexer
2	205	Transmit Reject Filter
3	294	"
4	232-1	"
5	232-2	"
6	232-1	"
7	232-2	"
8	031	Image Reject Filter
9	031	"
10	031	"
11	031	"
12	235	High Pass Filter
13	225	Dual Reject Filter
14	220	Single Reject Filter
15	090	Receive Multiplexer
16	490	Receive Duplexer

HY101	31796126	4-Way Power Splitter
2	126	"
3	126	"
4	126	"
5	197	2-Way Power Splitter
6	197	"
7	200	3 db Directional Coupler
8	108	3 db Hybrid
9	109	"
10	465	3 db Coupler (LHCF)
11	3 db Coupler (DZ-P85, Microlab)	

R101	Load (9200 Sage)	
2	"	
3	"	
4	"	
5	"	
6	"	
7	"	
8	"	
9	"	
10	"	
11	"	
12	"	
13	"	
14	"	
15	06023103	
16	Load (9200 Sage)	
17	"	
18	"	
19	31796136	Load
20	Load (9200 Sage)	
21	"	
22	31796330-3	Load
23	545	Attenuator
24	430-1	Load
25	430-1	Load
26	430-1	Load
27	430-1	Load
28	Pad (40375006-5)	
29	31796330-2	Load

RJ101	31796280	Rotary Joint
2	276	"
3	Rotary Joint (20-1533, MDL)	

T101	31796316	Transformer
2	"	"
3	"	"
4	"	"
5	"	"
6	"	"
7	"	"
8	"	"
9	31796346	Transformer

W101	31796330-1	Coax Cable
2	"	"
3	"	"
4	"	"
5	"	"
6	"	"
7	"	"
8	"	"
9	"	"
10	"	"
11	"	"
12	"	"
13	"	"
14	"	"
15	"	"
16	"	"
17	31796336-1	"
18	"	"
19	336-4	"
20	336-8	"
21	-	
22	336-5	"
23	336-6	"
24	336-7	"
25	4[illegible]	Wiring Cable
26	336-2	Coax Cable
27	336-2	"
28	336-3	"
29	336-3	"
30	096-5	"
31	096-8	"
32	096-6	"
33	096-4	"
34	096-1	"
35	096-3	"
36	096-7	"
37	096-2	"
38	Wiring Cable (WA-269-702, S/A)	
39	Wiring Cable (WA-360-702, S/A)	

WG101	31796365	Waveguide
2	368	"
3	366	"
4	367	"
5	364	"
6	396-1	"
7	356	"
8	363	"
9	361	"
10	358	"
11	359	"
12	-	
13		
14	371-2	"
15	-	
16	371-2	"
17	-	
18	362	"
19	361	"
20	360	"
21	373	W/G Transition
22	357	Waveguide
23	373	W/G Transition
24	-	
25	441	Waveguide
26	371-3	"
27	459	"
28	371-1	"
29	463	"
30	468	"
31	-	

S101	Switch (MA 7502 TNCA, Microwave Assoc.)
2	"
3	"
4	"

Index to Figure 4-3

SECTION V

COMPONENT DESIGN

5.0 GENERAL

This section discusses the engineering design parameters for each of the major components in the Cassegrain Feed System. Descriptive material such as found in the Technical Manual has been kept to a minimum. Emphasis is placed on electrical and mechanical requirements with coverage of the design milestones leading to the existence of hardware suitable for the requirements.

5.1 Feed Cone - The feed cone is 164 inches high, 110 inches diameter at the base and 71 inches at the top. At the top (with the antenna pointed at zenith) are the main and tracking feed horns. See Figure 5-1 for a cutaway view of the feed cone. Immediately below the main horn is the dual mode transducer that serves to separate the received signal into two orthogonal polarizations. Below this transducer the sum signal proceeds through the transmit-receive duplexer and transmit reject filter into the Maser preamplifier. The components are arranged to provide the shortest and simplest waveguide run between the main feed horn and the Maser, so that this path will contribute the least possible loss. The remaining components of the feed are arranged as appropriate.

The conical feed housing (Figure 5-2) is constructed entirely of aluminum except for stainless steel bolts and screws. The cone weight with all components except the Maser System is 2800 pounds. The structure will withstand 120 mph winds with the antenna at zenith and 70 mph winds with the 85-foot antenna in any other position. It will withstand a 24-inch snow load (8 lb/ft^3) or a one inch radial ice load with a 60 mph wind load while the antenna is at zenith.

An error in units of length conversion from feet to inches in the design calculations for wind loading resulted in portions

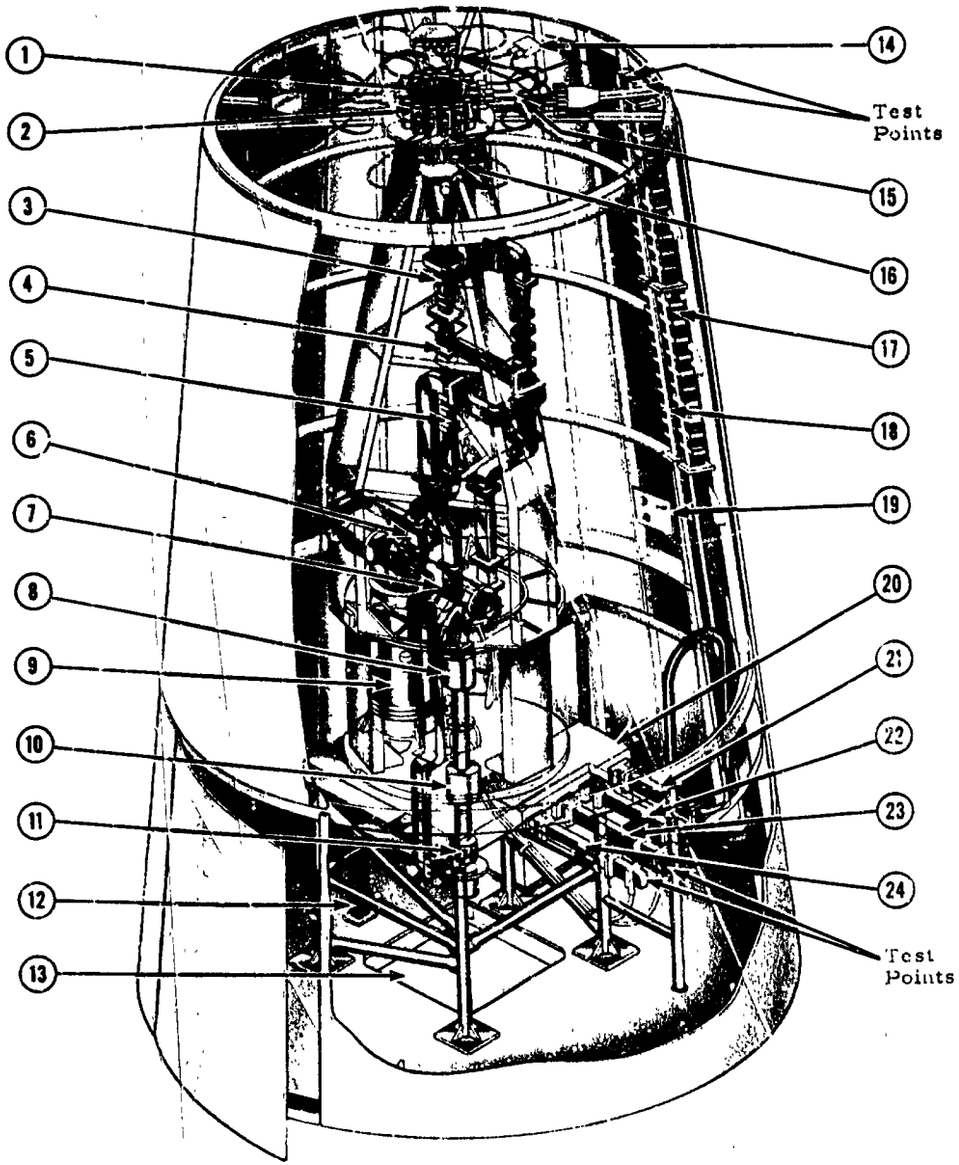

1. Communications Feed Horn (A101)
2. Tracking Array (A102-A117)
3. Dual Mode Transducer (T109)
4. Transmit Receive Duplexer (F101)
5. Transmit Reject Filter (F103)
6. 26 db Coupler (DC101)
7. Noise Source
8. Rotary Joint (RJ101)
9. MASER Amplifier
10. Rotary Joint (RJ102)
11. High Power Rotary Joint (RJ103)
12. Transmit Waveguide from Electronics Room
13. Crawl Thru Tunnel from Electronics Room
14. 3 db Directional Coupler (LY107)
15. 2-Way Power Splitter (LY105-LY106) 2 Places
16. 4-Way Power Splitter (LY101-LY104) 4 Places
17. Transmit Reject Filter (F104-F105)
18. Transmit Reject Filter (F106-F107)
19. Local Control Panel
20. Monopulse Converter
21. Image Reject Filter (F111)
22. Image Reject Filter (F110)
23. Image Reject Filter (F109)
24. Image Reject Filter (F108)

Figure 5-1. Cassegrain Antenna Feed Cone Assembly, Cutaway View

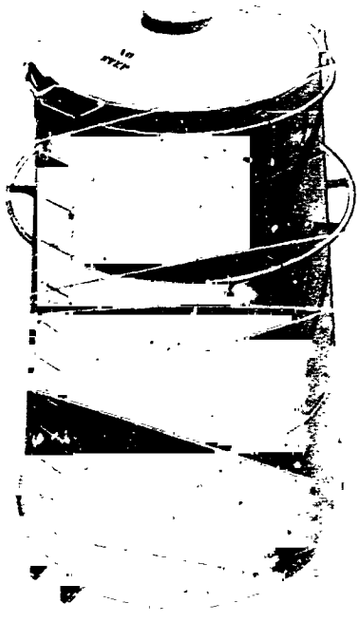

Figure 5-2. Feed Cone Housing

of the cone being designed and built to withstand wind loads in excess of these requirements by a factor of $\sqrt{12}$. However, when this error was discovered, no review was made to determine whether other aspects of cone design would withstand this same loading. Therefore, while parts of the cone would withstand the extra loading, it cannot be said that the over-all cone design is for wind loads in excess of the 120 mph and 70 mph winds described above.

The housing has four lifting lugs: two at the bottom and two at the top, located 180° apart. Two lugs are capable of supporting the fully loaded cone while it is being hoisted and rotated from the vertical to a horizontal position. The design provides an overload factor of 65% with respect to the yield point.

The inner surface of the cone housing has a 2-inch thick fibreglass insulation. All metal surfaces are painted with a semi-gloss white paint.

5.2 Subreflector - The subreflector diameter is frequently selected for minimum blocking of the main reflector aperture to minimize gain reduction and sidelobe increase. The approximate formula for minimum blocking is[1] $D_{s\ min} = \sqrt{2 F_m \lambda}$

[1] Peter W. Hannan, "Microwave Antennas Derived from the Cassegrain Telescope," IRE Trans. on Antennas and Propagation, Vol. AP-9, No. 2; p. 147; March 1961.

where

F_m = main reflector focal length, 36 feet

λ = wavelengths, 0.24 feet at 4.1 Gc

The result is 4.2 feet.

As stated previously, an 11-foot subreflector is used for this system without increasing the aperture blockage. This gives the advantage of permitting a broader feed primary pattern and reduction of the required feed aperture size.

The subreflector surface is made of doubly curved, continuous (no holes), aluminum panels. The support and stiffening structure behind the surface consists of eight radial aluminum tubes from the center hub to the outer support ring with numerous welded braces between the tubes and curved-Tee beams which form the support for the panels. The panels are fastened to the beams and outer ring with adjusting screws which allow for independent adjustment of the panels relative to the support structure. See Figures 4-1 and 5-3.

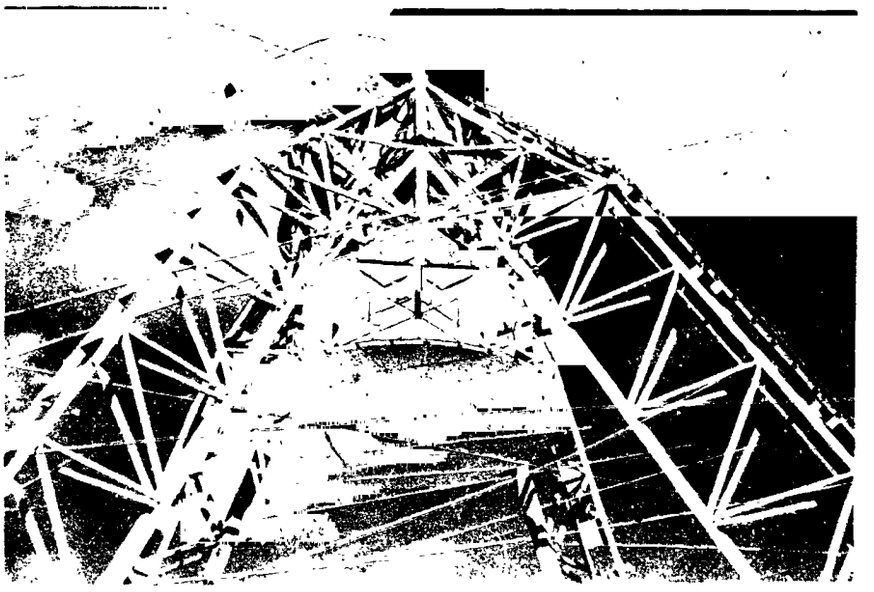

Figure 5-3. Subreflector Mounting to Quadrapod Structure

The reflector surface can be re-established and reset in the field by use of the template furnished. The specified surface accuracy is 0.030-inch root mean square (rms) average from the template using the method of least-square. Ninety-eight percent of the surface must be within 0.062-inch of the template with 0.1 percent of the surface allowed to deviate 0.093-inch. The actual subreflector had an rms and maximum deviation of 0.016-inch and 0.035-inch respectively before installation on the 85-foot antenna. The subreflector will withstand the same 24-inch snow load or one inch radial ice load in conjunction with a 60-mph wind load when the 85-foot dish is at zenith. It is designed to withstand 120 mph winds with the antenna at zenith and 70 mph winds with the antenna in any other position.

The subreflector is suspended from the quadrapod members as shown in Figure 5-3. The four 3-inch diameter lead screws will allow for ±8 inch of axial adjustment. The lead screws are attached to the subreflector with a ball and socket to allow for removal of the subreflector and replacement in the same location and attitude. The lead screws and sockets will allow for ±2° of angular adjustment. One full turn of opposite adjusting nuts in opposite directions results in a 9-minute change of subreflector axis.

The surface tolerance on the 85-foot paraboloid is 0.040 inch rms with respect to the "best-fit" paraboloid. With the hyperboloid also specified on an rms basis, the over-all effective rms tolerance is the square root of the sum of the squares of the individual reflector tolerances. Thus an 0.030-inch rms tolerance on the hyperboloid, results in 0.050 overall; the actual 0.016-inch rms subreflector surface results in 0.043-inch overall.

A simple formula for gain reduction caused by surface tolerance is[2]

$$\Delta G = 171\left(\frac{\sigma}{\lambda}\right)^2 \text{ db}$$

Based on this relation, the gain reduction is 0.052 db at 4.1 Gc and 0.125 db at 6.4 Gc with $\sigma = 0.050$.

5.3 Communications Feed Horn - The communications feed horn (see Figure 5-4) was developed using a half-scale model horn. The design employs a conical horn which tapers to a square throat for reception of orthogonal polarizations. The taper is long to minimize phase errors and a set of vanes near the mouth of the horn equalizes the E- and H-plane beamwidths. Radiation patterns were taken for four different sets of vanes. Patterns were taken for each set of vanes at four frequencies and in two planes. The 3- and 10-db beamwidths were measured on each pattern and are tabulated in Table 5-1. The best results were obtained with the 1/32" x 3/4" 40 vanes of case V. The E-plane patterns appear to be slightly overcompensated. However, the addition of the ring array for tracking reduced the E-plane beamwidth by the amount of overcompensation noted above. The E- and

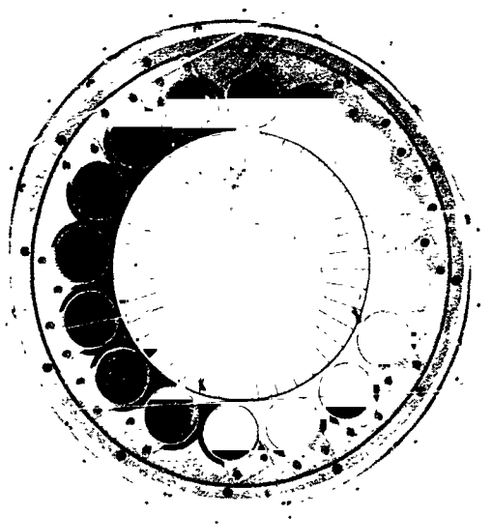

Figure 5-4. Feed Horn Surrounded by Tracking Array

[2] L. J. Anderson and L. H. Groth, "Reflector Surface Deviations in Large Parabolic Antennas," IEEE Trans on Antennas and Propagation, Vol. AP9, No. 5, pp 444-461; Sept, 1961.

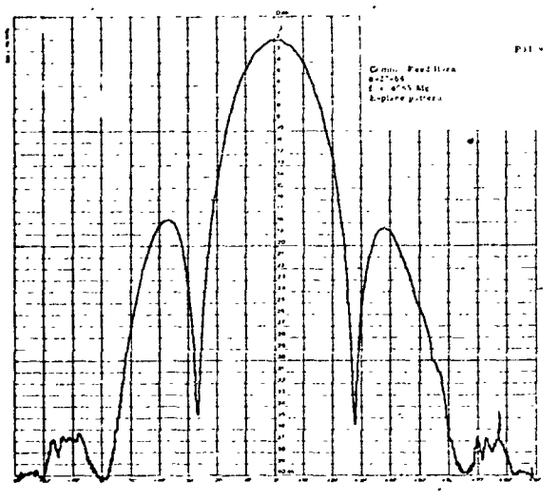

E-Plane Pattern 4085 Mc

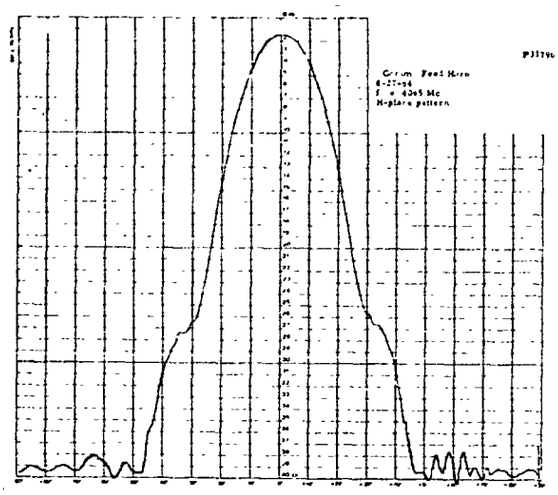

H-Plane Pattern 4085 Mc

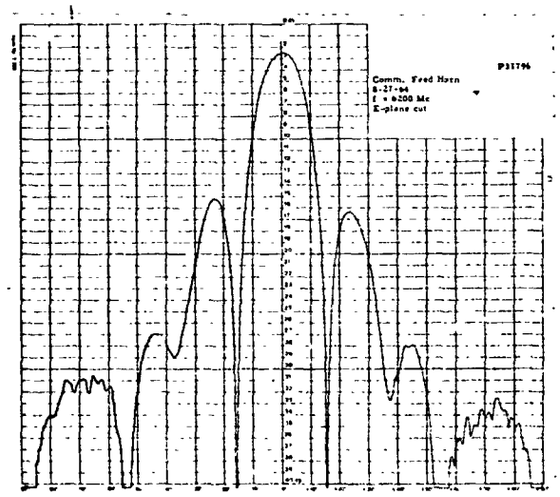

E-Plane Pattern 6200 Mc

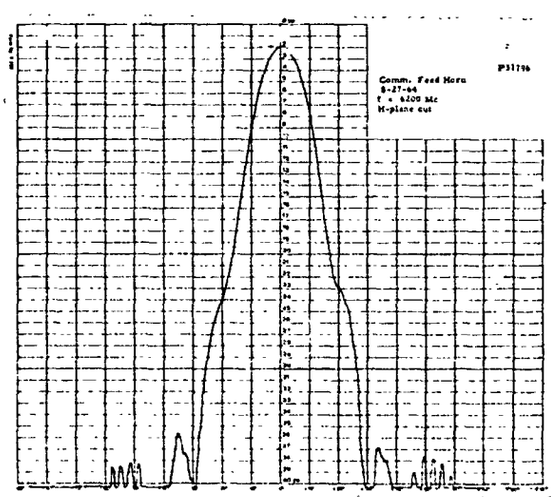

H-Plane Pattern 6200 Mc

Figure 5-5. Primary Patterns, E- and H-Plane, at 4085 Mc and 6200 Mc

Table 5-1. Half-scale Communications Horn Data

Freq	Plane	3 db Beamwidth					10 db Beamwidth				
		Case I No vanes	Case II 1/16x1/2 x44 *	Case III 1/32x1/2 x80	Case IV 1/32x1/2 x40	Case V 1/32x3/4 x40	Case I	Case II	Case III	Case IV	Case V
7984	E	17.8	21.6	21.9	20.9	24.7	31.0	36.4	35.8	34.6	40.7
	H	22.5	22.5	23.3	22.2	21.6	38	37.8	40.0	39.0	39.0
8388	E	17.5	21.9	20.3	19.6	23.9	30.5	36.0	35.0	33.6	37.9
	H	21.8	21.6	22.5	22.0	22.3	37.5	38.0	38.0	38.0	39.4
12038	E	12.5	14.3	14.6	13.4	14.8	21.6	23.9	24.0	23.8	25.8
	H	15.5	15.6	15.0	15.1	14	26.2	26.9	26.5	26.8	26.4
12600	E	12.1	13.7	13.9	12.3	13.9	20.9	21.3	22.5	22.4	24.2
	H	14.0	15.8	15.6	13.4	14.1	25	26.4	25.6	25.0	25.9

* Note: Information just below each case number indicates thickness, height and number of vanes used. In case No. 2 - 44 vanes 1/16 inch thick, 1/2 inch high [illegible]

H-plane primary patterns for the final horn installed in the ring array at 4085 Mc and 6200 Mc are in Figure 5-5.

An efficiency calculation was made to determine the percentage of the power radiated which would hit the subreflector at 4085 Mc. These calculations were based on the E, H, and 45° plane radiation patterns of the final horn. A planimeter integration method was used. The result was 80.6% for the 32° 11' angle subtended by the feed horn. The 19.4% spillover results in 0.94 db gain reduction.

The 1/2-scale horn with the vanes of case V was used for center of phase measurements. The center of phase lies between 0 and 1 inch behind the aperture in the E-plane at both 8150 Mc and 12260 Mc. The center of phase in the H-plane lies between 1 and 2 inches behind the aperture at the low frequency and 2 to 3 inches at the high frequency.

5.4 Feed System Weather Cover - A weather cover was required for sealing the radiating aperture at the top of the cone against the elements. The cover over the feed system had to be electrically transparent to the 4-Gc and 6-Gc signals but capable of withstanding snow and wind loading as well as hailstone impact without damage. It had to be low loss since its loss would add directly to the system noise temperature and it had to withstand the 20-kw radiated power without melting.

A thin mylar film was selected for its high tensile strength and low loss characteristics. The mechanical properties of a mylar window 0.002 inch thick and 15 inches in diameter were tested in the fixture shown in Figure 5-6. The film was secured between two aluminum rings and steel ball bearings 1/2 inch in diameter, weighing 8 grams, were dropped from heights up to 45 feet onto the film. The ball bearings were also thrown at the film with enough force to dent the aluminum. In all cases the film was stretched only in the immediate vicinity of the impact and never punctured. This test was believed to be more severe than hailstone impact. Calculations showed that the window should withstand

Figure 5-6. Impact Test, 0.002-Inch-Thick Mylar Window

the power densities to be radiated at the Rosman site. The on-site radiation test of 15 kw verified these calculations.

A VSWR check of the 0.002-inch-thick mylar film as a window showed a maximum VSWR of 1.07 in 0.900 inch square waveguide at the half-scaled transmit and receive frequencies. The VSWR is about half this value at the actual C-band frequencies for an identical thickness window.

After the 0.002-inch-thick mylar window was in use on the 85-foot antenna for several months it became brittle. Consequently, the mylar was replaced by 0.002 inch tedlar, a polyvinyl fluoride film with the same tensile strength as mylar but an expected life of 20 years in the elements.

5.5 Monopulse Tracking Array - The sixteen tracking array elements (see Figure 5-2) are designed to absorb both

circularly-polarized incident waves, one in the feed network and one in the horn array elements themselves. Following the three section capacitive pin and inductive iris phase shifter which converts the circularly polarized wave to linear polarization is a coax-to-waveguide probe backed by a short circuit septum. This probe receives one linear polarization and lets the other pass by and toward the back end of the horn where it is terminated in absorbing material.

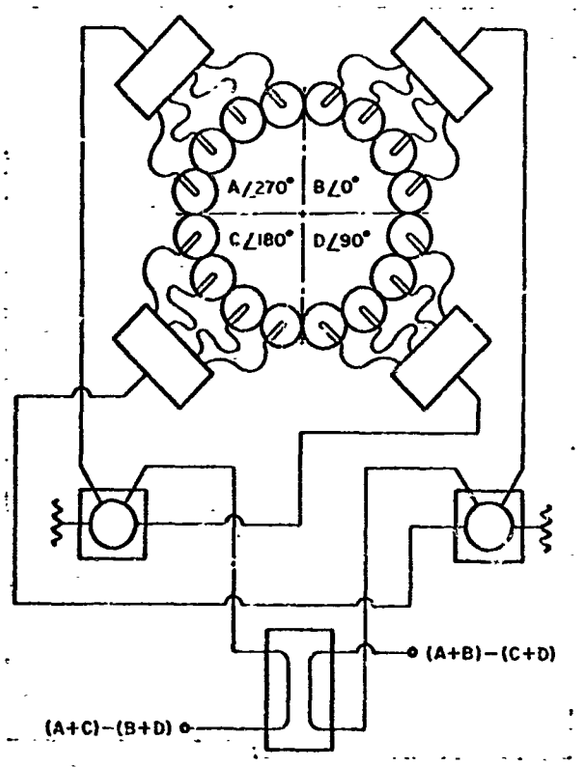

Figure 5-7. Tracking Feed

Since the coax probes are at right angles to the horn axis, each set of four horns was aligned with its probes at 90° relative to the adjacent groups. See Figure 5-7 for this horn arrangement and the feeding technique. The probe alignment causes a 90° phase progression from quadrant to quadrant.

The feed circuit of Figure 5-7 allows for this and has several unique features. First, all line lengths are equal so there is negligible frequency sensitivity from this cause. Second, the groups are connected in diagonal pairs which are inherently 180° out of phase because of the reversal of the probe positions; therefore, a simple power divider is adequate to generate the difference signal. These are "rat-race" type strip-line hybrids similar to those used for the four way power splitters. Thirdly, the difference channel null depths are not affected by the axial ratio of the horns (provided they are all identical) because the two sets of probes generating each difference pattern are responsive to similar modes passing through the

quarter-wave plates. It is not necessary that groups A and D have the same amplitudes as B and C which they probably would not have unless the axial ratios were in unity. Finally, a single 90° hybrid coupler can generate both azimuth and elevation difference patterns and provide good isolation between them.

There will be a phase shift in the tracking feed of 360° per revolution of the incoming polarization. A corresponding phase shift is added to the tracking sum signal when the communications horn is rotated to track the incoming polarization. The quarter-wave-plate phase shifter design, as used in the array horns, was used in the phase shifters for the sum and polarization error channels. Signals enter the rotating end of the joint through a probe from coaxial line or transition to round waveguide from rectangular waveguide. The linearly polarized signal passes from the rotating section to the stationary section through a noncontacting choke joint. The linearly polarized signal in the round waveguide is converted to circular polarization. The LCP signal is extracted for the sum and polarization error channels.

Due to the nature of circular polarization, the phase observed at the stationary probe is proportional to its angle relative to the rotating probe.

The ring array is used only for the tracking error channels since the sum pattern of the ring has nulls which fall well within the edge of the hyperbola. Another reason for picking up the sum channel in the main horn is the efficiency. Kelly[3] has calculated the efficiency factor of a ring and found it to be about half that of a solid aperture producing the same beamwidth. The error channel primary patterns are contained in Figure 5-8.

---

[3] F. J. Goebels, Jr., and K. C. Kelly, "Arbitrary Polarization from Annular Slot Planar Antennas," IRE Trans. on Antennas and Propagation, Vol. AP-9, No. 4; July 1961.

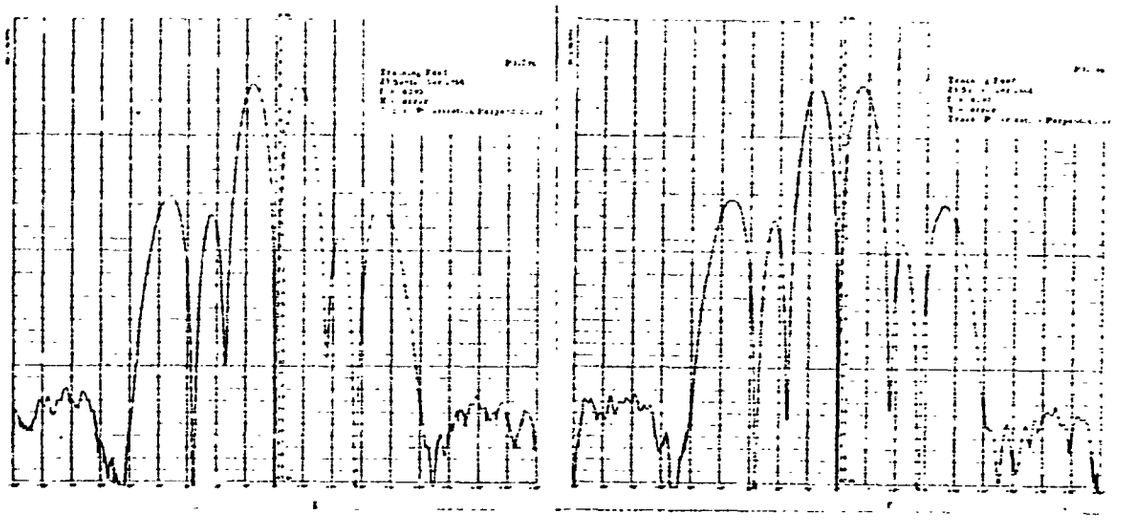

(a) X-error (b) Y-error

Figure 5-8. Error Channel Primary Patterns

5.6 Dual Mode Transducer - The dual mode transducer serves to separate the two orthogonal received polarizations into their respective waveguides. (See Figure 5-9.) The basic requirements are low VSWR and high isolation. The isolation is necessary for two reasons; one is to reduce the leakage of transmitted power into the orthogonal mode arm, and the other is to assure a deep null in the orthogonal mode arm when used for polarization tracking. The prototype transducer was built at half scale for X-band just as with the feed horn. The opening at the junction of the side arm was originally full size waveguide and presented a reactive discontinuity for the

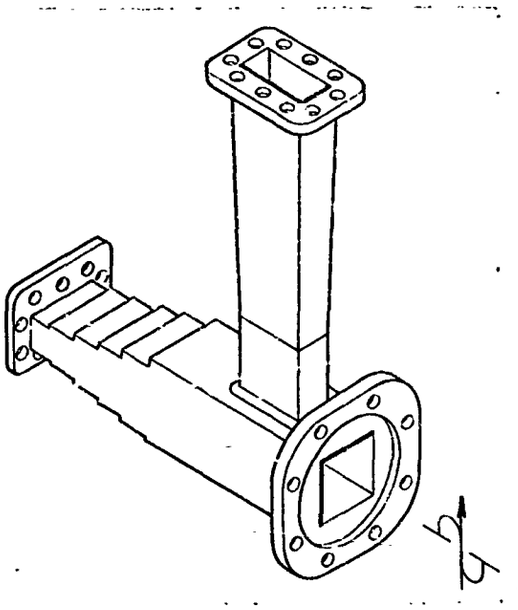

Figure 5-9. Dual Mode Transducer

straight-through modes giving a VSWR as high as 1.25:1. Consequently, the side arm was reduced to half-height waveguide and the maximum VSWR reduced to 1.09 in both the transmit and receive frequency bands. The isolation was greater than 30 db; it was found that a small screw at the corner of the square waveguide in the plane of the junction was effective in increasing the isolation of the orthogonal arm. This scale model was not further improved as the rectangular-to-square waveguide transition and septum presented accumulated mismatches.

The full size transducer had 1.10 VSWR or better over the receive band for both the through and orthogonal arms. The transmit band VSWR varied from 1.12 at 6000 Mc to 1.22 at 6400 Mc. These measurements were made with long tapered transitions to standard waveguide sizes with elimination of the errors introduced by the half-scale transitions. Impedance data showed that the transmit band could not be improved without seriously degrading the receive band.

The isolation between orthogonal ports was about 35 db with all efforts to improve this figure resulting in degradation of other transducer electrical properties.

The requirement for a pressurized waveguide system necessitated a window at or near the radiating aperture. This window is placed between the feed horn and dual-mode transducer. In this position it seals both the transmit/receive and the orthogonal waveguide lines. Also, the electric field intensity in the square waveguide is about 70% as large as in the rectangular waveguide. A study was made of various choke designs and mylar thicknesses to evaluate the effectiveness of the non-contacting flange and choke combination. Thin mylar was chosen because it had lower VSWR than 0.070 inch and 0.035 inch Dylec and Cymac windows. The results of the experiments indicate that a non-contacting choke flange is as good as a flange lapped to a number 8 finish. This statement is true for a frequency range where

the electrical lengths of the choke are between 0.2 λg and 0.3 λg where λg refers to the guide wavelength in the choke sections. Mylar thicknesses to 0.006 inch were used for the experiment.

A 0.002-inch-thick mylar window was high power tested in full-size waveguide. It ruptured at 8 kw CW when holding 6 psi waveguide pressure. Subsequently, a 0.007-inch-thick ruby mica window was used successfully at 20 kw CW. An inductive iris was used at the window interface to match the power from the horn into the through arm of the transducer.

5.7 Polarization Sensing and Rotation - The feed system contains a polarization alignment subsystem to determine the attitude of the satellite relative to the ground station by sensing the plane of polarization of the received signals and aligning the receiving antenna polarization to it. The beacon signals from the satellite are polarized parallel to the communications signal. Thus either beacon or communications signals could be used for polarization sensing; the beacon signal is used since detected amplitude is not affected by data transmission. The requirement of 0.1 degree resolution in polarization tracking necessitates use of the cross polarized null since signal level varies sinusoidally with polarization angle and the peak of a sine function is relatively flat.

The null sensing and polarization tracking is implemented by reception of both the desired and the cross polarized signal. These signals are extracted from the feed horn by the dual mode transducer. The sum signal is then amplified by the Maser and TWT before injection into the phase compensating rotary joint and extraction from the rotating assembly to the monopulse converter for conversion to 136 Mc. The polarization error signal is fed from the dual mode transducer directly to the waveguide input rotary joint, thence to the converter. The polarization receiver is a dual channel phase-lock receiver which compares phase and amplitude of the sum and polar-

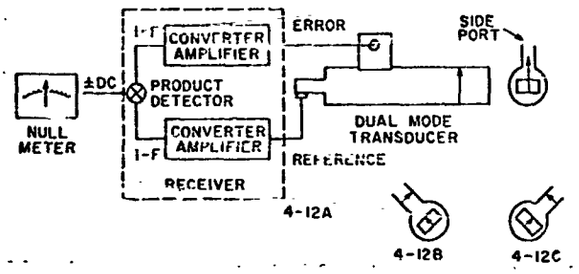

Figure 5-10. Polarization Sensing Equivalent Circuit

ization error signals to generate an error indication so that the receiving horn can be rotated into alignment with the satellite polarization.

The dual mode transducer provides for 180° phase shift in the polarization error signal across the polarization null; hence the receiver can indicate sense as well as amplitude of polarization misalignment. See Figure 5-10.

The block diagram for the receiver installed in the feed system is shown in Figure 1 of Appendix I of this report. The system is required to provide polarization alignment information with a threshold signal level of -102 dbm. The sum signal is amplified 30 db by the Maser and 28 db by the TWT before being put into the converter. The polarization error signal has no amplification prior to the converter. Because the 0.1 db alignment accuracy depends upon phase and amplitude stability between sum and polarization error signals every effort must be made to prevent leakage between channels in the converter. Field tests were made with 20 db attenuation prior to the converter and the additional 38 db attenuation at the receiver input. It was found that null fill-in was occurring from the sum signal into the polarization error channel. Presumably, the same sort of null fill-in was occurring in the X- and Y-error channels. Consequently, the 38 db sum channel excess gain was removed prior to the converter by insertion of a 30 db coupler and 28 db pad in place of the original 20 db pad.

Ideally, the dual mode transducer would have infinite isolation between ports so that polarization misalignment could be indicated by signal level in the polarization error channel relative to the sum channel. This polarization misalignment angle θ is related to

the signal level below the sum channel peak by the function -db = 20 log sin θ.

The requirement for 0.1° polarization alignment accuracy corresponds to a 55 db null --- a null depth which could not be achieved in the dual mode transducer because of leakage from the sum signal to the polarization error waveguide port. This leakage signal within the transducer is of unknown phase relative to the sum signal and is about 35 db below the sum signal.

The unwanted signal in the error channel can be eliminated by adding a small signal from the sum channel of the correct phase and amplitude for cancellation. This would be accomplished by addition of a directional coupler in each channel of the receiver with an attenuator and phase shifter between the two couplers. This could be done anywhere before AGC is generated, that is before the 136 Mc signal is injected into the present receiver or within the receiver itself at 136 Mc or 45 Mc.

After the calibration procedure, the present receiver can be used for precise polarization alignment so long as the leakage or unwanted signal does not change amplitude or phase relative to the sum. This is unlikely to happen in the feed system since all components are waveguide or semi-rigid coaxial cable. The signal leaves the feed cone after being converted to 136 Mc so that the effect of cable movement over the antenna axes should have minimum effect upon accuracy.

5.8 Transmit Diplexer

5.8.1 Dual Reject Filter - The dual reject filter was required to handle 20 kw CW power in either of two modes, the transmission mode as for the power from the transmitter No. 1 or the rejection mode as for the transmitter No. 2 power as shown in Figure 5-11. The requirement was for 40 db rejection of the transmitter No. 2

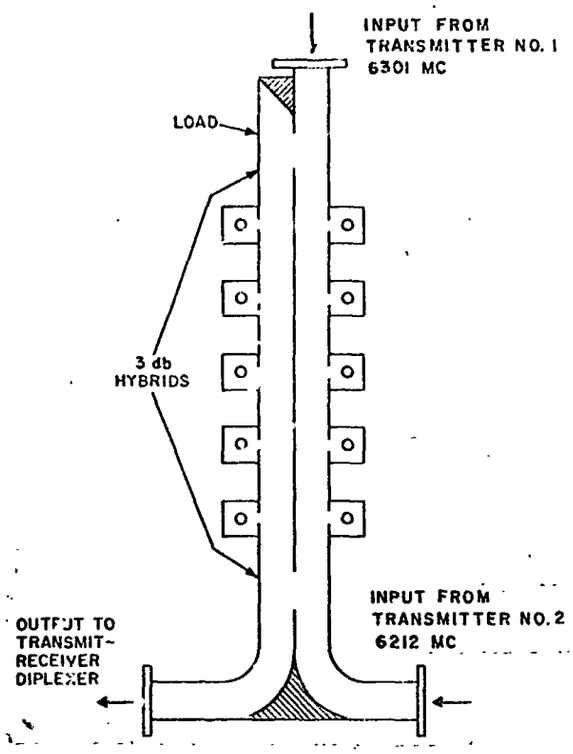

Figure 5-11. Transmit Diplexer Schematic

power over a 25 Mc bandwidth with a minimum insertion loss at the transmitter No. 1 frequency. The system design requires that the No. 1 frequency be above No. 2.

The original project requirements were for three (3) dual reject filters at 6019 Mc, 6108 Mc, and 6212 Mc. This requirement was later modified to one unit at 6212 Mc. The Rosman II system was to operate with 8 kw CW at 6212 Mc from the FM transmitter and 1 kw CW at 6301 Mc for the SSB transmitter.

The dual band-reject filter was designed for a 0.001 db ripple bandwidth of 86 Mc and a 40 db rejection bandwidth of approximately 40 Mc. This required loaded Q's of 160 to 386. The design consists of coupled cavities in the H-plane of the waveguide. These cavities are resonant at the rejection center frequency and are shunt inductances at the higher pass-through frequencies. Consequently, capacitive buttons were used to match the waveguide to this pass-through frequency.

The problem area encountered in this design was power handling capability in the reject mode. The prototype filter was tested at 100 kw pulse power and successfully rejected this power. However, a test of this model at CW resulted in voltage breakdown in the first cavities at 6,500 watts. This breakdown was from the cavity tuning screw in the top of the cavity to the bottom wall. Consequently, the two front cavities of each filter section were redesigned with 0.872 inch

height instead of the original 0.795 inch. Two 1/4-40 tuning screws were installed in each cavity instead of the previous single 10-32 screw. Each screw was one-fourth cavity width from the wall so that no screw was in the maximum field region of the cavity. The screw ends were rounded and polished to minimize the voltage gradient. The cavity length was designed for minimum screw penetration. This configuration handled 13,000 watts CW prior to arcing. Voltage breakdown calculations indicated the filter should withstand 61 kw. This, coupled with the fact that the filter withstood approximately 100 kw under pulse conditions, indicated quite conclusively that the filter was inherently capable of handling the required power.

The tuning screws were then eliminated from the first two cavities and the tuning accomplished by deforming the walls of the resonator. The filter now handled 20 kw CW in either the pass-through or reject mode.

The initial test indicated that the temperature of the first reject cavities would reach about 100°C at 10 kw CW input with forced air cooling. Consequently, water cooling tubes were installed on the filter and the maximum cavity temperature kept at 100°C with 20 kw CW power in the reject mode.

High power tests were conducted at Rosman with both transmitters operating simultaneously, the SSB transmitter at 6301 Mc and 4.5 kw output, the FM transmitter at 6212 Mc and 10.5 kw output. The entire system handled the 15 kw successfully, an excess of 6 kw above the normal operation of 9 kw total power, i.e. 8 kw FM, and 1 kw SSB.

5.8.2 Three-Element Filter - The input from transmitter No. 1 (Figure 5-11) is isolated from transmitter No. 2 by the 3 db hybrid directivity and dual filter symmetry of approximately 35 db. Consequently, an additional filter is needed to give the required 40 db

isolation - a filter that rejects the No. 1 frequency to be located between the dual filter and transmitter No. 2. This filter must have 5 db rejection over the 25 Mc bandwidth of transmitter No. 1. These filters were furnished for 6108 Mc, 6212 Mc, 6301 Mc, 6390 Mc, and 6405 Mc. The present Rosman II installation will use only the 6301 Mc filter, i.e. the SSB transmitter frequency. The filter was designed to give the minimum of 5 db rejection at $f_o \pm 12.5$ Mc with minimum insertion loss at the lower frequency of 6212 Mc. The design loaded Q is 282 to 500; the 0.001 ripple bandwidth is 155 Mc. The insertion loss of the 6301 Mc unit was 0.040 db at 6225 Mc. The filter used three H-plane coupled cavities for rejection which looked like shunt capacitance at the lower pass-through frequency. An inductive post was used opposite each cavity for impedance matching. No high-power problems were encountered in this design as the cavities were not resonant to the 20 kw CW pass-through frequency.

5.9 Transmit-Receive Duplexer - The transmit-receive duplexer consists of a common junction, high-pass filter in the transmitter arm to reject the receive band, and a band-reject filter in the receiver arm to reject the transmit band. (See Figure 5-12.) The high-pass filter consists of a section of waveguide with 1.240 x 0.797 inner dimensions which provides at least 10 db per inch at 4.2 Gc. The insertion loss at 6.0 - 6.3 Gc (the originally specified frequencies) of a ten inch section was less than 0.1 db and the VSWR was less than 1.05.

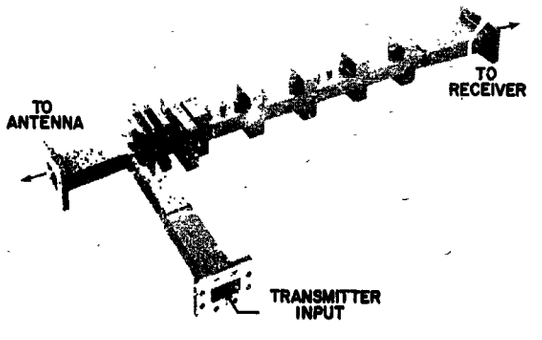

Figure 5-12. Transmit-Receive Duplexer

The band-reject filter presented problems in terms of getting a sufficiently broadband (low Q) reject element as required for low-loss duplexing. For an

insertion loss of 0.01 db at 6.15 Gc, a loaded Q of 5 was needed. Narrow wall (H-plane) cavities on both sides of the guide gave loaded Q's near the required value of 5 but the excitation of the TE_{20} mode caused poor rejection at the high end of the band. Broadwall (E-plane) cavities on both sides of the guide gave the same Q of approximately 5 with less TE_{20} excitation. The waveguide size was subsequently reduced to 1.680 x 0.872 inner dimensions to prevent TE_{20} propagation at 6.3 Gc.

Problems were encountered in matching the band-reject filter at 4.0 - 4.2 Gc without reducing its required rejection of 100 db at 6.0 - 6.3 Gc. The filter cavities acted as shunt inductances requiring shunt capacitance for matching. Design of the matching vanes suspended across the waveguide and supported by the narrow walls was done empirically. The interaction of matching capacitance and cavity loaded-Q was the complicating factor in this matching.

At the time the deliverable filters were being tuned, the frequency requirement was changed from 6.0 - 6.3 Gc to 6.0 - 6.425 Gc with 85 db rejection allowable between 6.0 and 6.1 Gc. Since it was desirable to use the existing hardware, the filters, though designed for equal element tuning, were stagger-tuned to give the required frequency shift. Considerable difficulty was encountered in keeping the higher order mode spikes below 100 db and the procedure required many slight tuning adjustments alternately in the 4 Gc and 6 Gc bands before the requirements could be met. The resultant filter had the required isolation with 0.09 db maximum insertion loss in the 4.0 - 4.2 Gc band.

5.10 Transmit Reject Filter - The transmit reject filter used in the orthogonal receive arm is identical electrically to the filter described in Section 5.9 as part of the transmit-receive duplexer. It has the same 85 db rejection over the band 6.0 - 6.1 Gc and 100 db between 6.1 Gc and 6.425 Gc. During high power tests at Rosman with the FM transmitter at 8 kw output at 6212 Mc, and the SSB transmitter at 1 kw output at 6301 Mc, the output at the Maser flange and

orthogonal receive arm was below -45 dbm. This indicates at least 115 db isolation at these frequencies.

The transmit reject filters on the X- and Y-error channels are the same design with two filters in series for each channel to give a minimum rejection of 180 db over the 6.0 - 6.425 Gc band.

5.11 Monopulse Converter - The Monopulse Converter, located on the floor of the feed cone, converts the sum, polarization error, and X- and Y-error signals from 4 Gc to 136 Mc. The four-channel converter contains four balanced crystal mixers and four 136 Mc preamplifiers which use a common power supply. One problem in development was mating the mixer and image-reject filter so that the reactive image load presented by the filter would enhance rather than hurt noise figure. Spacers were inserted between the prototype image-reject filter and the MDL Type L24334 mixer until the noise figure was optimized across the 4.0 - 4.2 Gc frequency band. The four deliverable filters were fabricated and tuned to the same amplitude specifications as the prototype; however, their phase slopes were different with the result that two channels had noise figures of 11 db or higher at certain frequencies within the band. This problem was solved by adding a spacer to the channel where this was physically possible without any component rework, and adjusting the tuning screw between the mixer and first iris on the filter in the other troublesome channel.

The mixers, as delivered from MDL, used matched pairs of IN23F crystals. After installation of the feed system at Rosman, the crystals were replaced with IN23G's for a noise figure improvement of about 0.3 db. The noise figure was 8.? db or less for all channels in the 4.1 - 4.2 Gc band of beacon signals. Noise figure was measured for crystal currents of 0.5 ma - 1.0 ma with 0.75 ma giving the best overall performance.

Another problem area in the converter development was matching of the 136 Mc mixer to the preamplifier. Cable length between the two components and preamplifier input tuning were adjusted for optimum noise figure.

The preamplifiers used in the converter are Rantec Model EPV-904-3. Each provides approximately 30 db amplification and has a 1-Mc passband centered at 136 Mc. The preamplifier noise figure is approximately 3 db. These amplifiers use two GE 7768 ceramic tubes. These tubes were chosen in preference to all-solid-state amplifiers because of possible saturation or non-linearity effects which might occur from leakage of transmit power into the converter. The preamplifier requires +200 vdc, -6 vdc, and +6.3 vac. This power is supplied by a single type rpm 201-200, ACDC Electronics, Inc. unit.

Interchannel isolation within the converter was specified at 55 db. For the acceptance tests at Rantec, four isolated local oscillator inputs were not available. Consequently, the 136 Mc output from each channel was measured with signal and L.O. only on one channel. Negligible leakage was expected prior to the mixers since all inputs were waveguide. The measured isolations were greater than 60 db except for the X-error to Y-error which measured 56 - 59 db. After installation of the feed system at Rosman, the measurements were repeated with local oscillator operating on each channel. The measured isolations were less than previously measured but all were 55 db or greater except for X-error to Y-error which measured 43 - 45 db. Since this far exceeds the approximate 20 db isolation within the tracking feed itself, no effort was made to determine whether the leakage occurred from the local oscillators or between cables and preamplifiers within the converter box itself. It should be mentioned that the isolation between signal input and local oscillator ports of the mixers is about 17 db. This would result in 34 db isolation if the local oscillators are not isolated. However, isolators were installed at the L.O.

output ports in the Electronics Room and each should give at least 20 db isolation for a total of 54 db minimum isolation between L. O. channels.

5.12 Receive Multiplexer

5.12.1 ATS Quadriplexer - The original multiplexer requirement was for separation of four channels 25 Mc wide and centered at 3992 Mc, 4051 Mc, 4120 Mc, and 4179 Mc. Twenty-eight db isolation was required at ±60 Mc from any of these center frequencies.

The four-channel multiplexer (of which only the 4120 Mc and 4179 Mc channels are used) is of the directional-filter type. Four-cavity filters, in circular waveguide, attach in series along the input rectangular waveguide. (See Figure 5-13.) Power is extracted from the input waveguide by each filter from signals only within its own frequency band. Signals at other frequencies pass down the input waveguide to the other filters or the load on the end. The filters are directional in that a forward traveling wave in the input waveguide, excites a wave traveling toward the output port in the output waveguide. A backward traveling wave in the input waveguide excites an oppositely circularly polarized wave, which excites a wave traveling into the load opposite the output port. Half-height rectangular waveguide was used at the input and output in order to achieve coupling to the cavities with convenient iris sizes. Transitions to type N coaxial connector formed the actual four-channel multiplexer input and outputs.

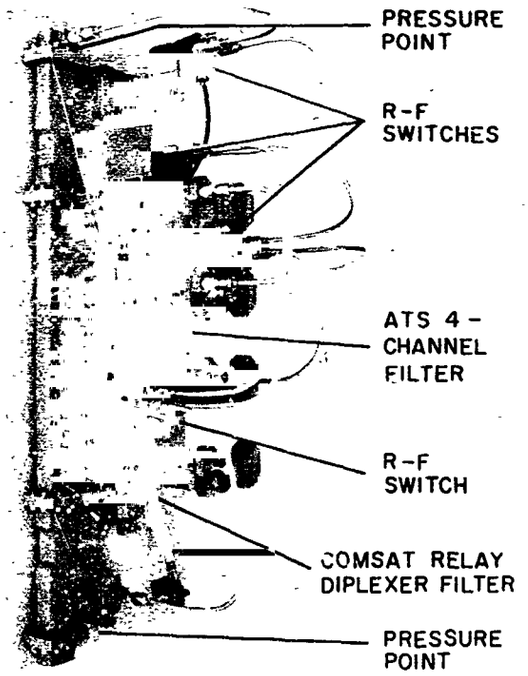

Figure 5-13. Receive Multiplexer Assembly

The prototype filters were three-cavity units. They could only marginally meet the 28 db rejection at f_o ±60 Mc. The 0.1 db ripple specification over the 25 Mc bandwidth, together with the requirements for operation over the 50°F to 100°F temperature range, necessitated redesign for four cavities in each directional filter. The four-cavity unit was considerably more difficult to tune; however, it gave a 28 Mc 0.1 db bandwidth, 83 Mc 30 db bandwidth, and 42 db rejection at f_o ±60 Mc with an f_o insertion loss of 0.3 db. Tests of the 4120 Mc four-cavity unit over the required temperature range indicated a 25.4 Mc 0.1 db bandwidth, 80.6 Mc 30 db bandwidth, 0.3 db insertion loss at f_o and maximum VSWR of 1.1:1.

The difficulty in tuning the directional filters required monitoring of three parameters during the tuning procedure. These parameters are insertion loss through the filter, return loss on the input waveguide, and power not extracted from the input waveguide by the filter. Each cavity used five tuning screws, the fifth being used to optimize the filter axial ratio.

5.12.2 Comsat/Relay Diplexer - The diplexer for the 4067-4123 Mc and 4137-4183 Mc bands is constructed in WR-229 waveguide. It consists of two 3 db short slot couplers, a dual band-pass filter for the lower bands, and a single band-pass filter for the upper band. The dual filter is a 10-element bandpass filter with a Tchebyscheff design for 0.01 db ripple over the 56 Mc band. There is a requirement for 25 db adjacent channel rejection at the 4123 Mc and 4137 Mc band edges. Bandpass filters are required because of the sharp rejection skirts required between bands. The major problem with the dual filter was in identically tuning the two sections to give low VSWR for the rejection mode and low insertion loss for the pass-through mode. Low insertion loss requires identical phase lengths between the two 3 db short slot couplers.

The single bandpass filter for 4137 to 4183 Mc is an 8-element, 0.01 db ripple, Tchebyscheff design.

N type coax to WR-229 waveguide transitions completed the input and two output connections for the diplexer and provided for connection to the switch matrix.

Insertion loss through the dual filter from input to output N connectors was 0.56 db at band center to 1.15 db at the band edges. Insertion loss for the high frequency channel varied from 0.74 db at band center to 1.30 db at 4137 Mc.

5.12.3 Receive Multiplexer Switching Circuit - The filter and switch arrangement to provide for reception of either ATS channel or either Comsat/Relay channel by Receiver 1 or Receiver 2 is as shown in Figure 5-14. The switches are Microwave Associates Type 7502, Type N, coaxial switches. An individual switch had typically 1.10 VSWR over the 4.0 - 4.2 Gc frequency band. The switches require 115 volt 60 cycle power for switching and automatically disconnect the power supply when switching is completed. At completion of switching an indicator circuit closes to allow for remote monitoring of switch position.

The cables are 3/8 inch semi-rigid foamflex. Careful matching of the cables was required to achieve the 1.3 VSWR requirement through the filter, cable, and switch combination. Insertion loss through the system was 1.6 to 2.2 db depending upon filter losses.

The electronic circuitry for switching and monitoring are detailed in the Feed System Instruction Manual.

5.13 Maser Preamplifier System - For a complete description of the Maser Preamplifier System, refer to the Goddard Space Flight Center Manual.

5.14 Collimation Tower Equipment - The Rantec furnished equipment for the Bald Knob collimation tower consisted of a 4-foot

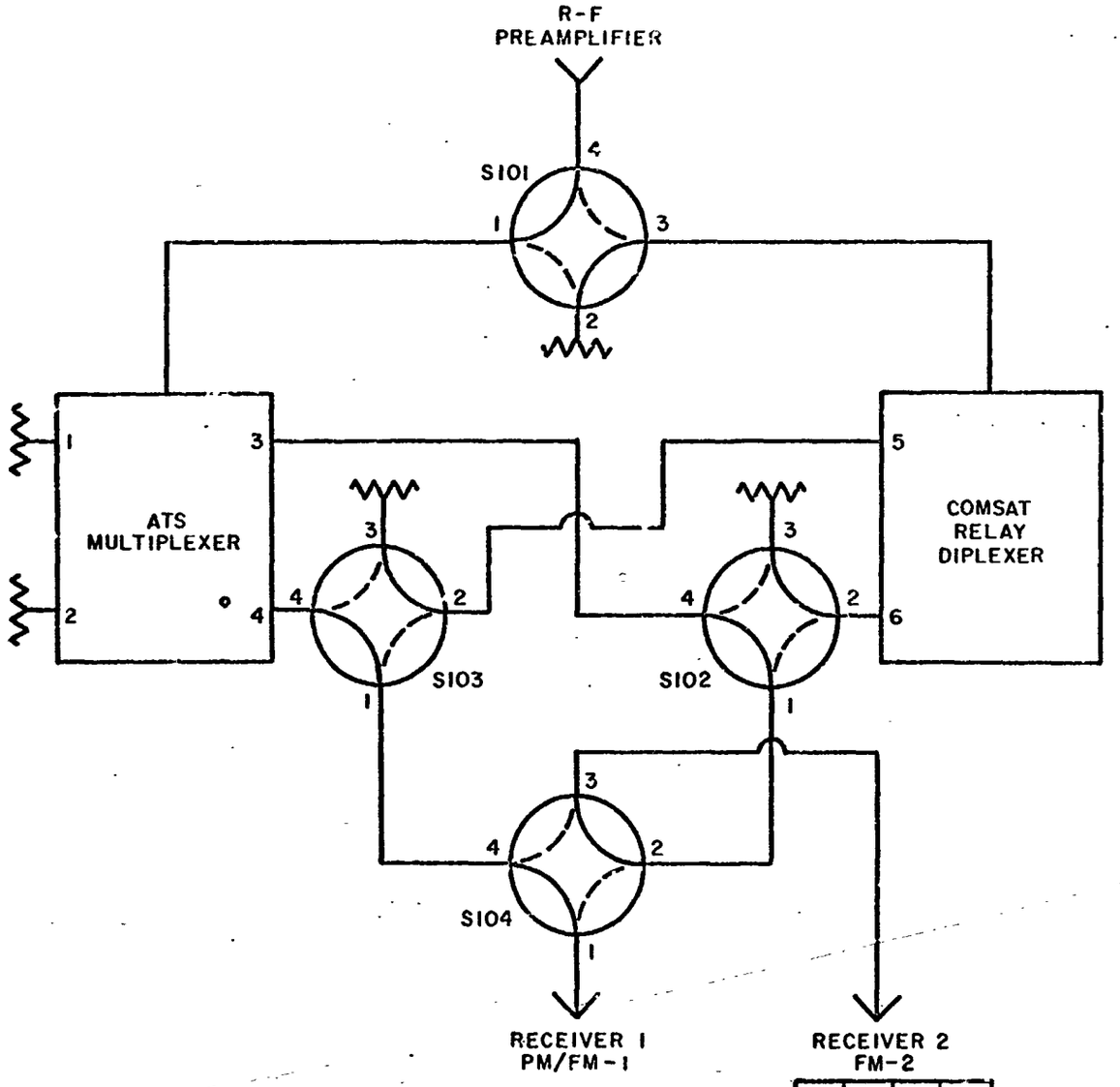

			S101	S102	S103	S104
a	RCVR 1, CHAN 3	RCVR 2, CHAN 4	0	0	0	1
b	RCVR 1, CHAN 4	RCVR 2, CHAN 3	0	0	0	0
c	RCVR 1, CHAN 5	RCVR 2, CHAN 6	1	1	1	0
d	RCVR 1, CHAN 6	RCVR 2, CHAN 5	1	1	1	1

0 AS SHOWN = B
1 OPPOSITE = C

Figure 5-14. Receiver Multiplexer Switching Circuit

parabolic dish for 6 Gc and a 6-foot parabolic dish for 4 Gc together with the associated polarization positioners. A 5-foot square optical target was furnished and mounted on the collimation tower but was never used because the optical cage on the 85-foot antenna was mounted 180° from the originally specified location. As a result, NASA extended the collimation tower from 102 feet to 120 feet and mounted another optical target that was used for the Cassegrain system boresighting.

Keuffel and Esser Co. 71-3250 Coincidence Levels were mounted on each of the collimation tower antennas to indicate vertical polarization. The setting of these levels was done at Rantec by use of GSFC furnished calibrated horns. The calibration and polarization tracking was accomplished on a 30-foot range with precautions taken to suppress reflections. This matter is further discussed in Section 6.4 of this report.

SECTION VI

SYSTEM OPERATION

6.0 GENERAL

This section of the report discusses the electrical performance characteristics of the Cassegrain Feed System in the 85-foot antenna and elaborates on the data contained in Acceptance Test Report, Rantec No. 31796-ATR-1.

6.1 Secondary Patterns - Sum - The secondary patterns and gain measurements were taken using the Bald Knob collimation tower which is at an elevation angle of 5° from the 85-foot antenna and at a distance of 4.2 miles. The lower portion of the 85-foot dish is shielded from the collimation tower by trees on a ridge about 300 feet from the 85-foot antenna. The illumination at the bottom of the 85-foot dish is down about 16 db from that at the top because of this shielding; it is approximately as shown in Figure 6-1. This illumination is an average obtained from a grid of illumination intensity measurements taken at 10 foot intervals over the face of the 85-foot dish when pointed at the collimation tower. The measurements were made at 4195 Mc.

The antenna E- and H-plane patterns at 4195 Mc and 6200 Mc are shown in Figure 6-2. These patterns should be compared to the theoretical E- and H-plane secondary patterns that were calculated at 4179 Mc and a 45° pattern at 6200 Mc. These patterns are shown in Figure 6-3. The theoretical patterns have approximately 20 db sidelobes and are computed from the primary pattern illumination taper without any corrections for aperture blockage.

The effect of aperture blockage on sidelobe level can be approximated by Jensen's[4] formula

[4] Paul A. Jensen, "Designing Cassegrain Antennas," Microwaves, December 1962, pp. 12-16.

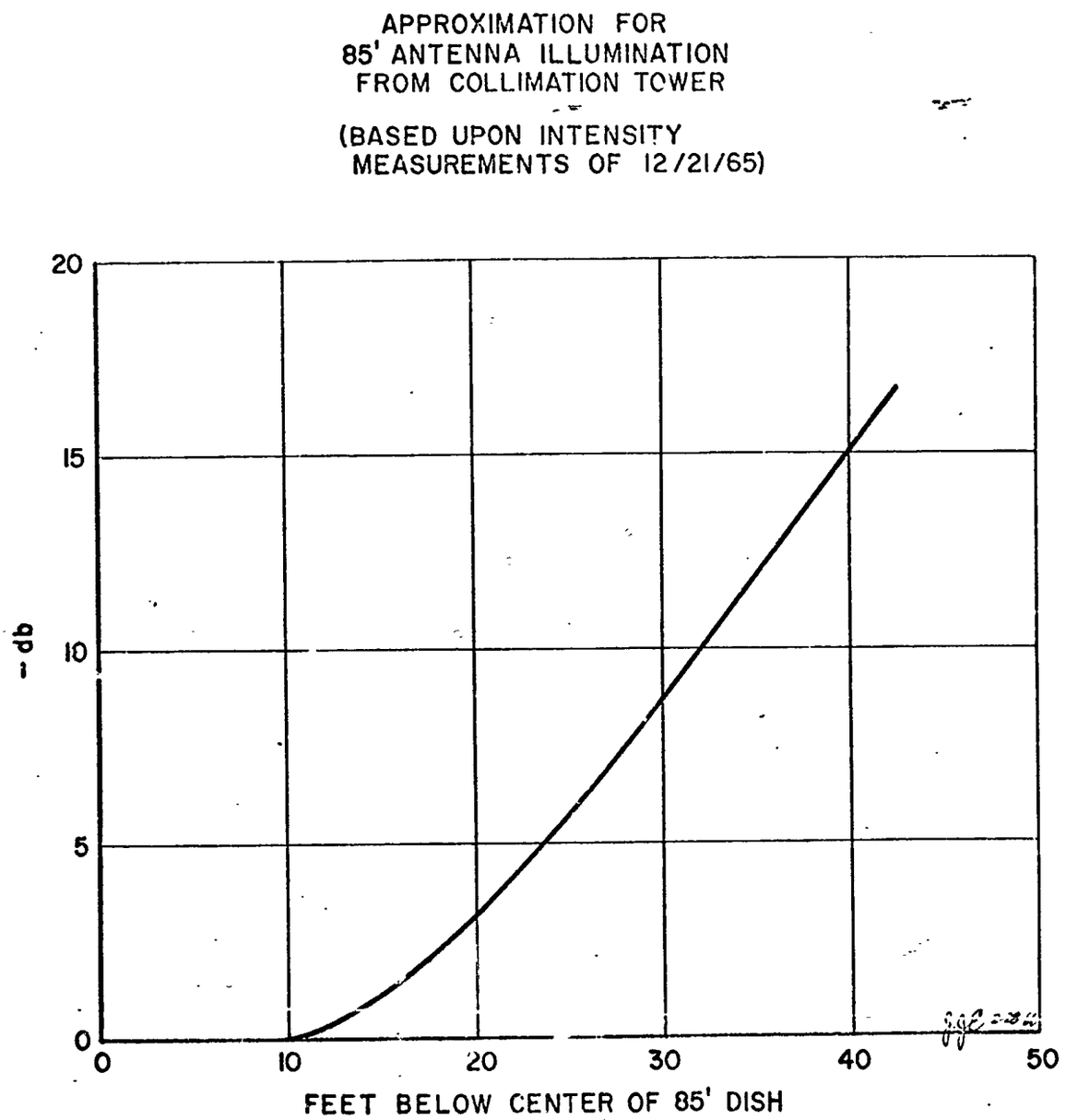

Figure 6-1. Approximation for 85-foot Antenna Illumination from Collimation Tower

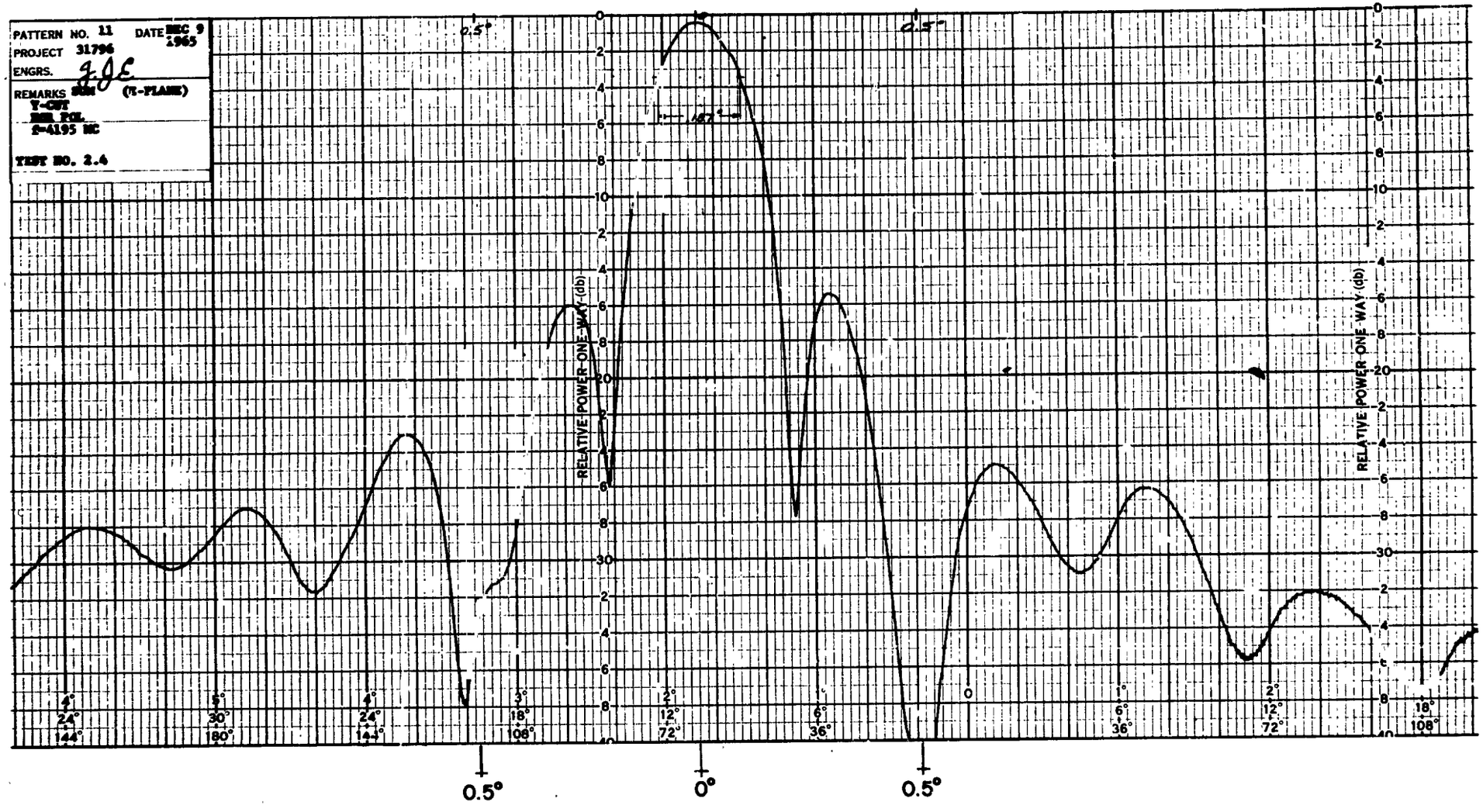
PATTERN NO. 11
DATE DEC 9 1965
PROJECT 31796
ENGRS. JDE
REMARKS SUM (H-PLANE)
T-CUT
MIR. POL.
f=4195 MC
TEST NO. 2.4
0.5°
0.5°
RELATIVE POWER ONE-WAY (db)
RELATIVE POWER ONE-WAY (db)
4° 24° 144°
5° 30° 180°
4° 24° 144°
3° 18° 108°
2° 12° 72°
1° 6° 36°
0
1° 6° 36°
2° 12° 72°
3° 18° 108°
0.5°
0°
0.5°

1-3-61

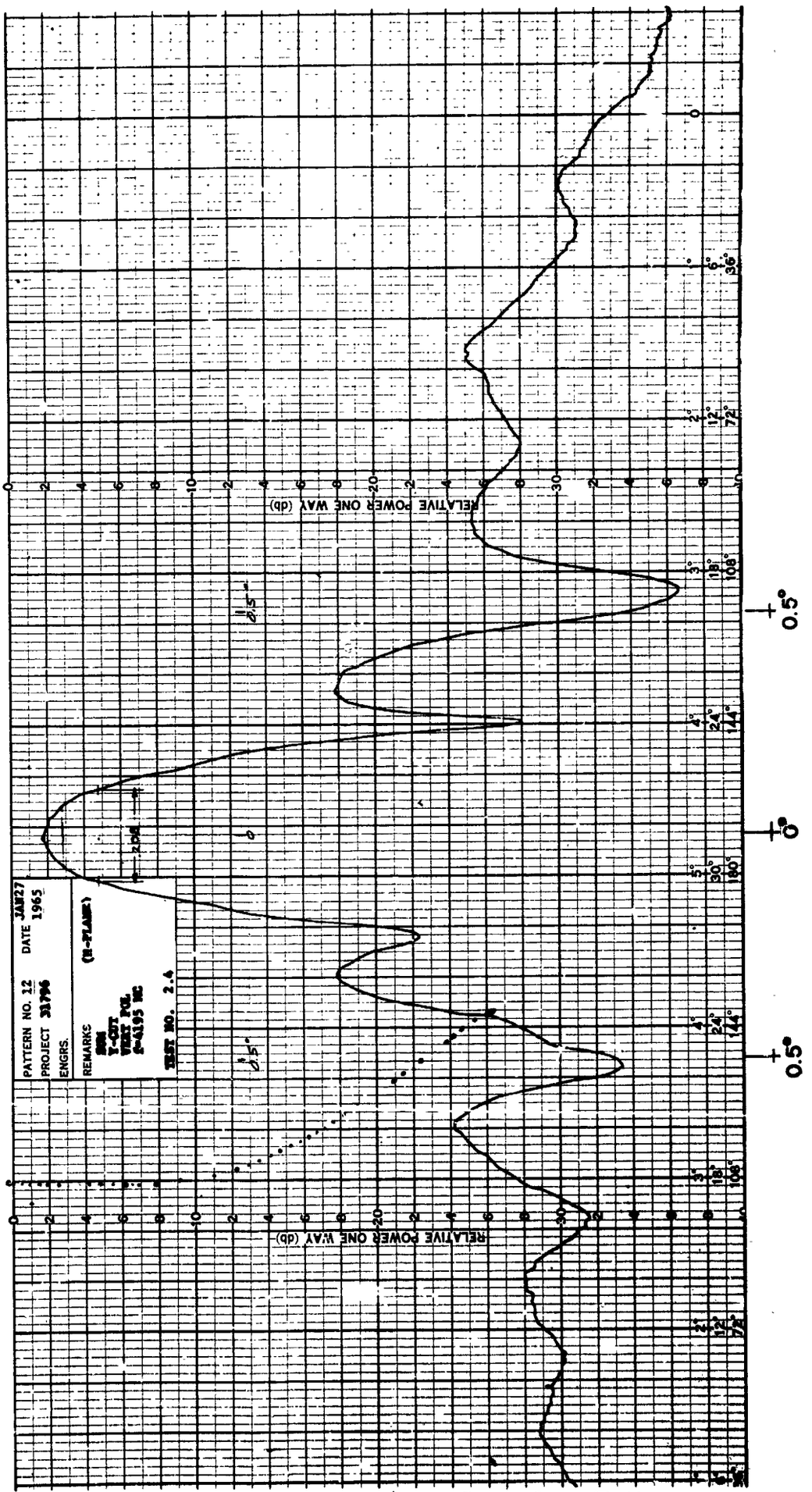

Figure 6-2. Secondary Patterns, Sum -- E- & H-Plane at 4179 Mc (Sheet 1 of 2)

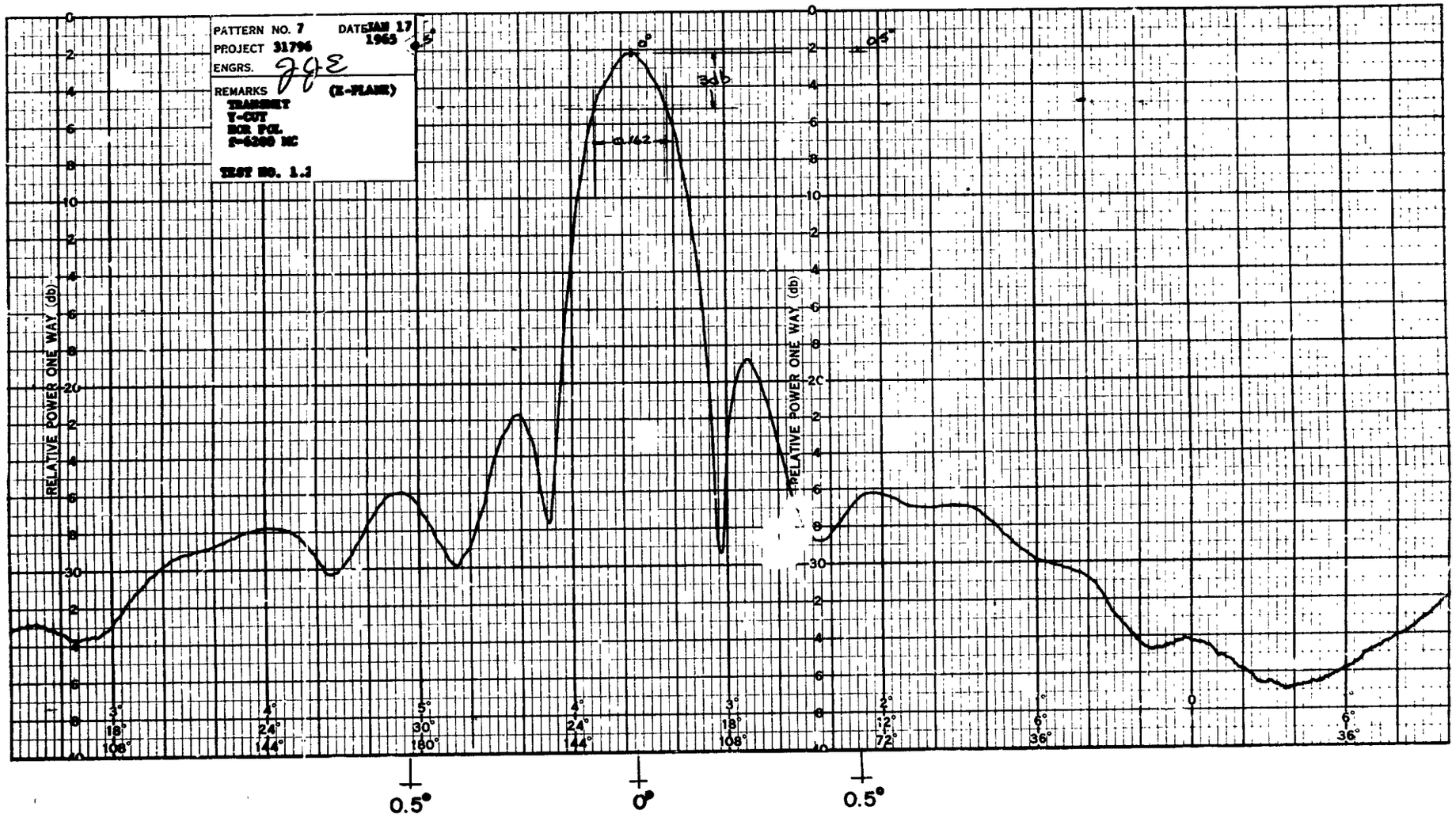
PATTERN NO. 7
DATE JAN 17 1965
PROJECT 31796
ENGRS. JJE
REMARKS (E-PLANE)
TRANSMIT
T-CUT
HOR POL
f=6200 MC
TEST NO. 1.1
RELATIVE POWER ONE WAY (db)
0°
3db
.762
.95°
0.5°
0°
0.5°

1-69

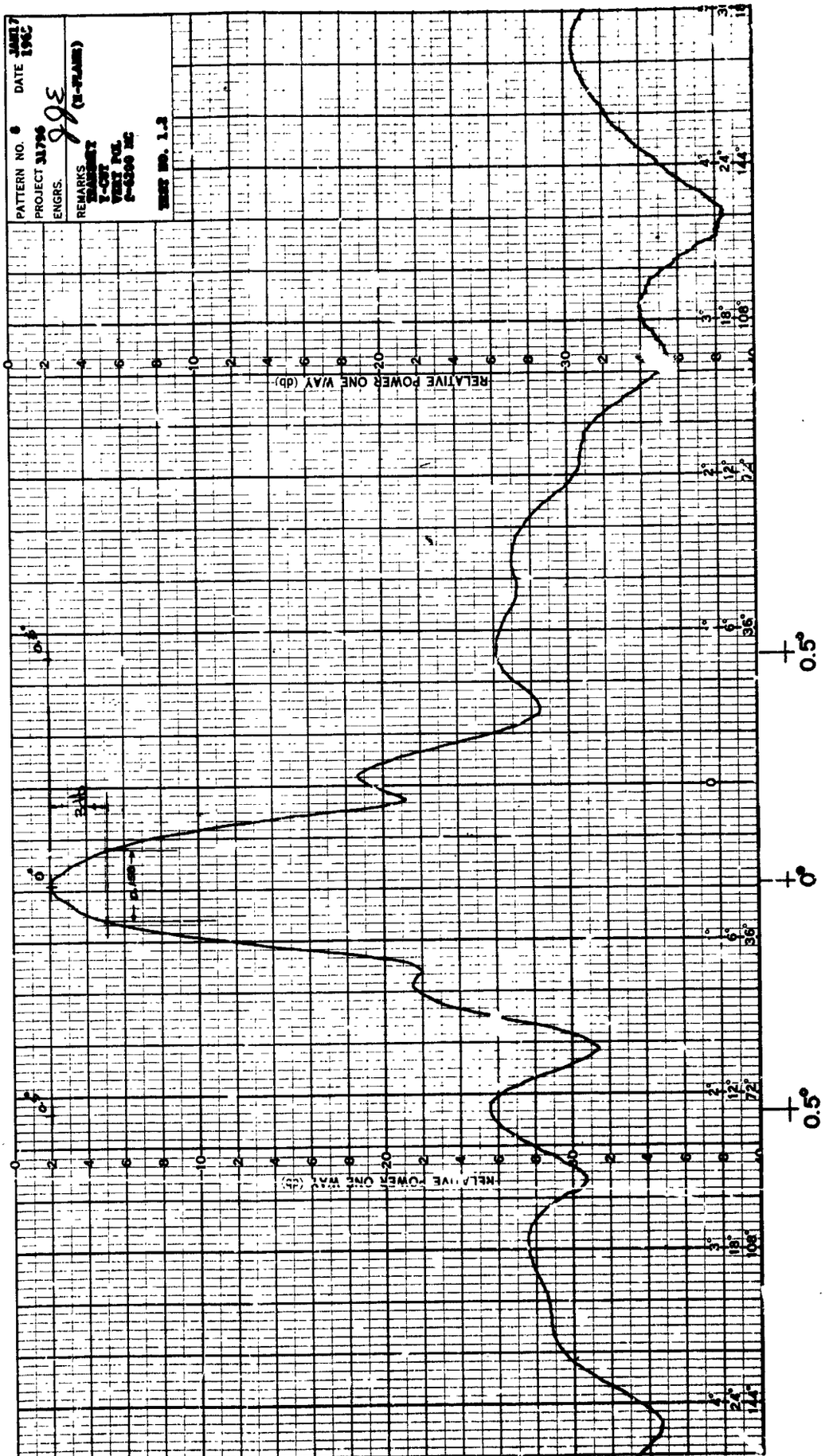

Figure 6-2. Secondary Patterns, Sum -- E- & H-Plane at 6200 Mc (Sheet 2 of 2)

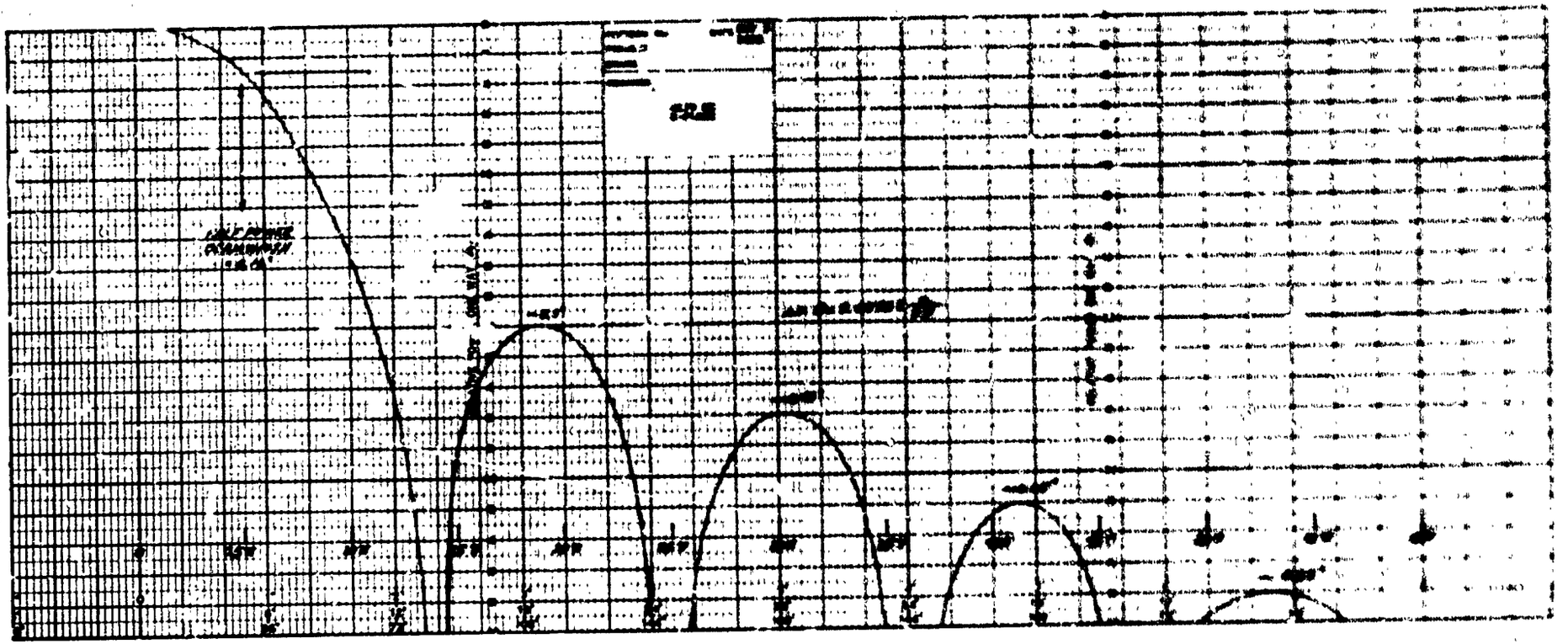

U in Radians

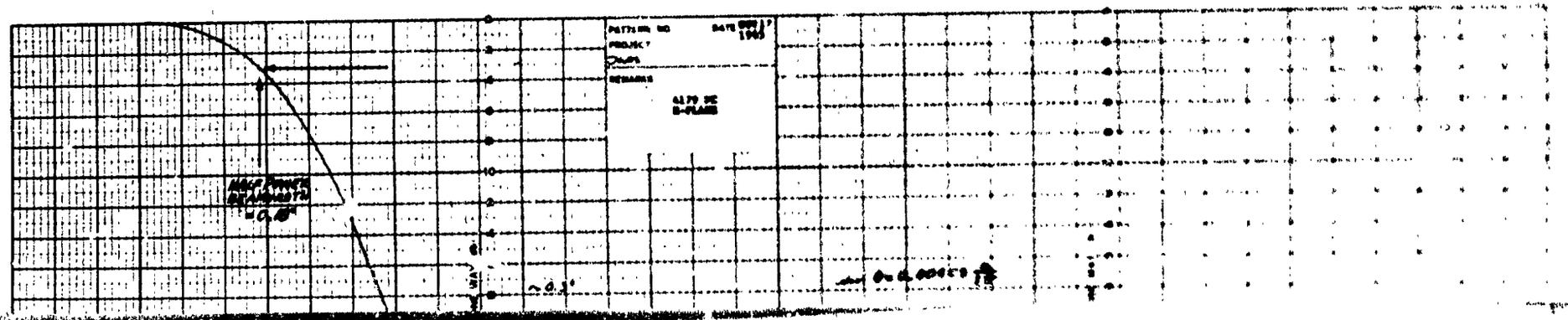

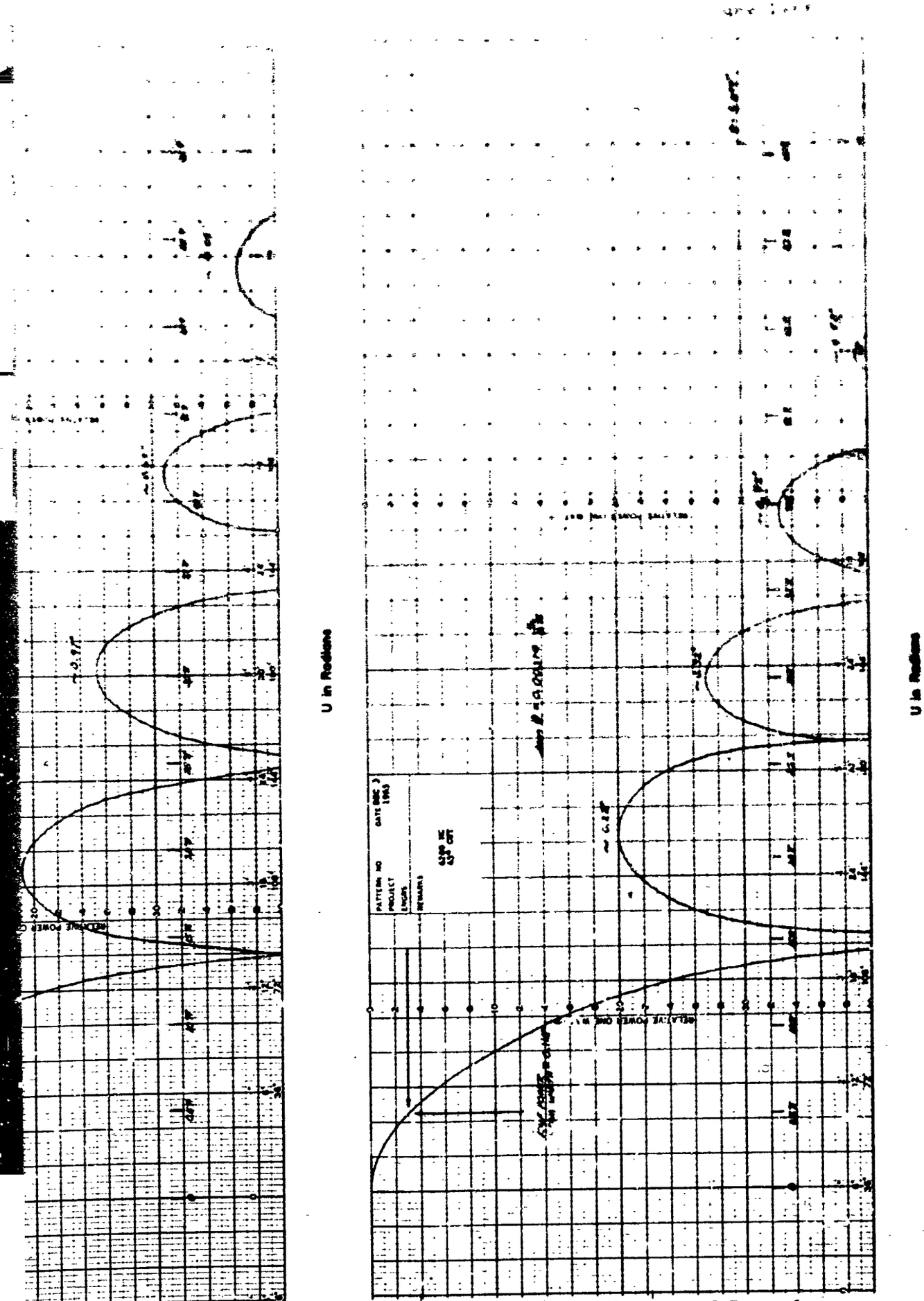

Figure 6-3. Calculated Secondary Patterns, Sum (courtesy of Goddard Space Flight Center)

$$\text{New sidelobe level} = 20 \log \left[\frac{\frac{E_s}{E_m} + B^2}{1 - 2B^2} \right]$$

where E_s/E_m is the sidelobe to main beam voltage ratio for the unperturbed antenna and the factor B is the ratio of subreflector to main dish diameter. For the 11-foot subreflector diameter and 20 db sidelobes without blockage the new sidelobe level will be 17.2 db. This sidelobe level is optimistic since the actual system the eight-foot square prime feed box and quadriped legs add additional blockage.

Allowing an additional 2% for this blockage brings the calculated sidelobe level to 16.4 db. It is believed that illumination phase errors caused by ground reflections would account for the measured 15 - 15.5 db sidelobes. The illumination intensity vertical profile revealed 3 db variations in signal strength above the tree level, a result of these ground reflections.

The R-F characteristics of the Communications Feed System are summarized in Table 6-1.

The secondary patterns shown in Figure 6-2 are Y cuts or essentially horizontal cuts. The Bald Knob collimation tower is located roughly northwest of the Rosman site; the antenna coordinates for Bald Knob are approximately X = -82.7°, Y = +48.8°. Thus, a Y cut is actually not horizontal but is tilted 7.3° to the horizontal.

An X-cut would be a vertical cut only if the collimation tower were located straight east or west of the 85-foot antenna. On the other hand, if the collimation tower were north or south of the site, an X-cut would just be a rotation of the 85-foot antenna, not a cut through the main beam. Since the Y-angle is so great for the Rosman antenna, the X-cut is an arc through the main beam with the beam appearing to be 1.5 times as large as actual. Furthermore, the X-cut is an in-and-out antenna motion such that the received field is not cut

Table [illegible]. R-F Characteristics

Frequency	4195	6[illegible]	Mc
Gain	58.5	61.2	db
Efficiency	55	47	percent
Beamwidth			
H-Plane	0.208	0.158	degree half power
E-Plane	0.187	0.162	degree half power
First Sidelobe	-16	-17	db
Other Sidelobes	-22	-24	db

but is probed along the line between the collimation tower and 85-foot antenna. This field probing and the effect of ground reflections causes the X-patterns to be non-symmetrical with 12 db sidelobes on one side of the main beam, 20 db on the other side, with the beam measuring 1.5 times wider than actual. For these reasons only the Y-patterns are included in Figure 6-2.

6.2 Antenna Gain - An integration for gain was made at 4195 Mc using the following equation from Silver.[5]

$$G_m = \frac{4\pi}{\lambda^2} \frac{\left| \int_A F(\xi, n)\, d\xi dn \right|^2}{\int_A \left| F(\xi, n) \right|^2 d\xi dn}$$

where

G_m is the gain for constant phase over the aperture

$F(\xi, n)$ is the illumination function over the aperture as a function of ξ and n, the coordinate points within the aperture.

[5] S. Silver, "Microwave Antenna Theory and Design," McGraw-Hill Book Co., Inc., 1949, p. 177.

An average of the E- and H-plane primary patterns of Figure 6-2 was used for $F(\xi, n)$ and the calculation made without and then with the effect of the illumination shielding.

The gain was 60.5 db and 59.6 db respectively or a reduction of 0.9 db caused by the tree shielding. These calculated gains do not take spillover into account. A planimeter measurement of the primary pattern indicates 19% spillover, or 0.92 db gain reduction.

The estimates for other factors contributing to loss in gain are shown in Table 6-2. Multipath effects between the 85-foot antenna and collimation tower antenna produced 3 db variations in the vertical profile signal strengths. The resultant phase errors are estimated to produce 0.3 db gain reduction. The aperture blockage figure of 0.3 db for the hyperboloid was obtained from Jensen's formula for estimated gain loss:

$$\text{Gain Loss} = 20 \log (1 - 2B^2)$$

Table 6-2. Antenna Gain at 4195 Mc

Gain (by integration from primary pattern)	60.5 db
Spillover past subreflector	-0.94
Phase errors (including collimation tower illumination)	-0.30
Spillover past 85-foot antenna	-0.15
Hyperboloid aperture blockage (increased SLL)	-0.30
Quadripod legs blockage (increased SLL)	-0.10
Surface Tolerances	-0.05
Feed Loss	-0.15
Theoretical Gain	58.53 db
Shielding by Trees	-0.90
Near Field Gain Reduction	-0.30
Theoretical Gain to be Measured	57.33
Actual Measured Gain	56.89
Difference	0.44 db

The theoretical gain of 58.53 db is believed to be closer to the actual gain than the 58.39 db calculated by using the measured gain and correcting for tree blockage and near field gain reduction. This belief is based upon three things.

First, the measured gain corrections totaling 1.4 db have not taken the aperture illumination phase errors into account and the near field gain reduction is 0.3 db only if the Cassegrain system is focused at infinity but is 0 db if the system is focused at the collimation tower.

Secondly, the wide variation between the gain standard of 17.57 db and the approximate 58 db to be measured is a large source of error.

Thirdly, the limitations imposed by the measurement technique used could account for 3 db variations in measured gain. The gain measurements were taken by pointing the standard gain horn from the lip of the 85-foot dish at zenith toward the collimation tower and then comparing this signal level to that received by the 85-foot antenna when pointed at the collimation tower. Measurements were made with the standard gain horn at three different locations on the lip of the dish. However, as mentioned previously, 3 db signal variations were found in the vertical profile of signal strength at the 85-foot antenna. It was not possible to probe the field vertically during the gain measurements; this could be a large source of error in the measured values.

The theoretical calculated gain of 58.53 db as in Table 6-2 represents an overall efficiency of 55.2%.

A similar analysis can be made at the 6.0 to 6.4 transmit frequency as in Table 6-3. A field intensity probe was not made in this frequency band but the loss through the trees blocking the aperture is expected to be greater at the higher frequency due to the increased dielectric loss of the trees. The aperture taper efficiency of

Table 6-3. Antenna Gain at 6200 Mc

Gain (uniform illumination)	64.52 db
Aperture Taper Efficiency - 67.13%	-1.74
Spillover past subreflector	-0.60
Phase Errors (including collimation tower illumination)	-0.30
Spillover past 85-foot antenna	-0.05
Hyperboloid Aperture Blockage (increased SLL)	0.30
Quadriped Legs Blockage (increased SLL)	0.10
Surface Tolerances	-0.12
Feed Loss	-0.05
Theoretical Gain	61.20 db
Shielding by Trees	>-0.90
Near Field Gain Reduction	-0.75 db max
Theoretical Gain to be Measured	59.55
Actual Measured Gain	60.49
Difference	>0.94 db

67% was taken from Sciambi;[5] spillover taken from planimeter integration of primary patterns. Other factors are estimated. It should be noted that the 0.75 db near field gain reduction is a maximum figure which can be used only if the Cassegrain system is focused at infinity, but the correction goes to zero if the system is focused at the collimation tower. The theoretical gain of 61.2 db corresponds to an overall efficiency of 46.8%. This lower efficiency at the transmit band is essentially caused by the taper efficiency of only 67% compared to 87% for the receive band.

6.3 Secondary Patterns - Monopulse Tracking

6.3.1 General - The X- and Y-error secondary patterns are shown in Figure 6-4. It will be noticed that the X-error pattern appears wider than the Y, is non-symmetrical, and seems to have a shallow null depth, about 14 db. These effects are explained in

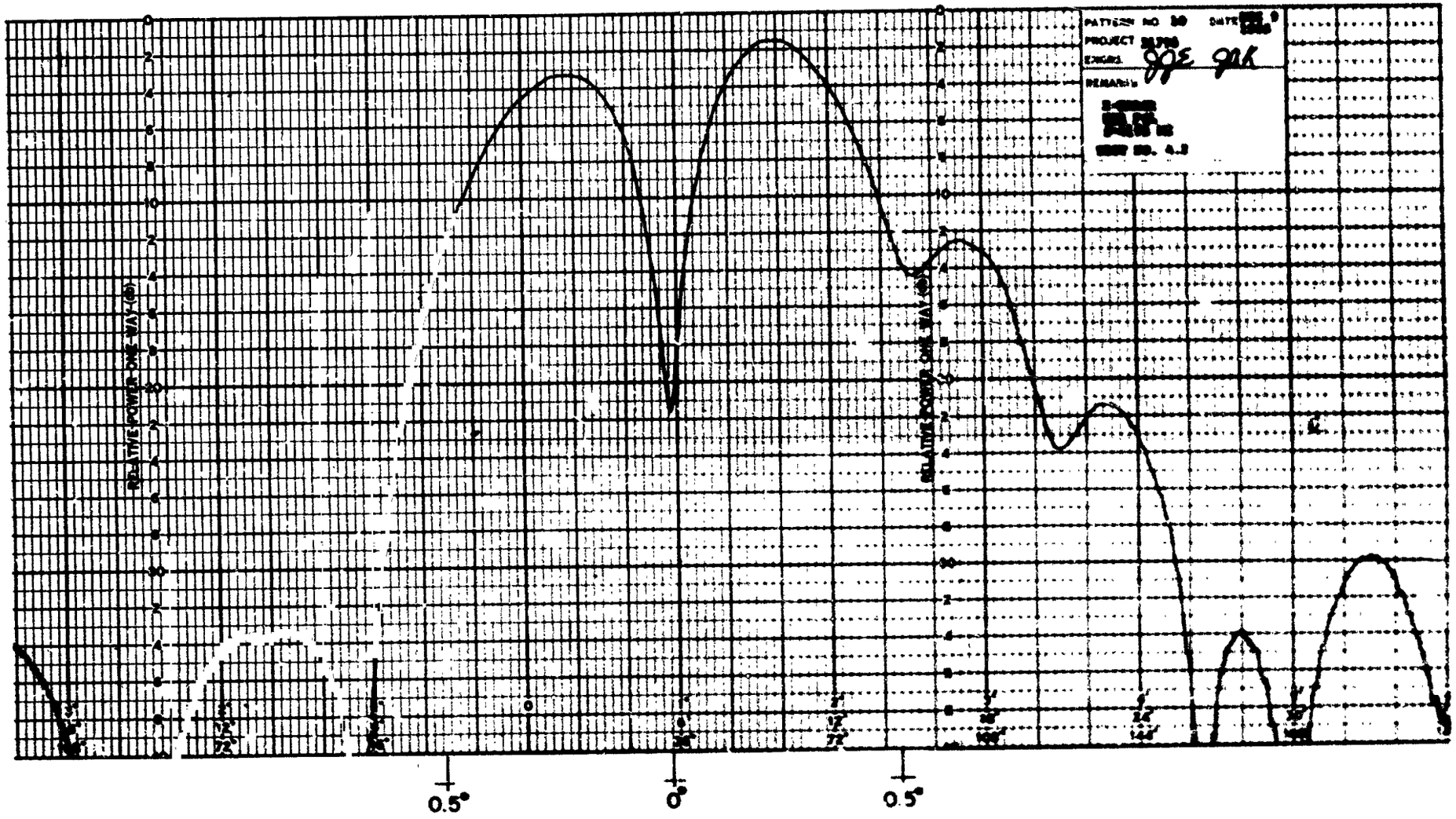

11-9

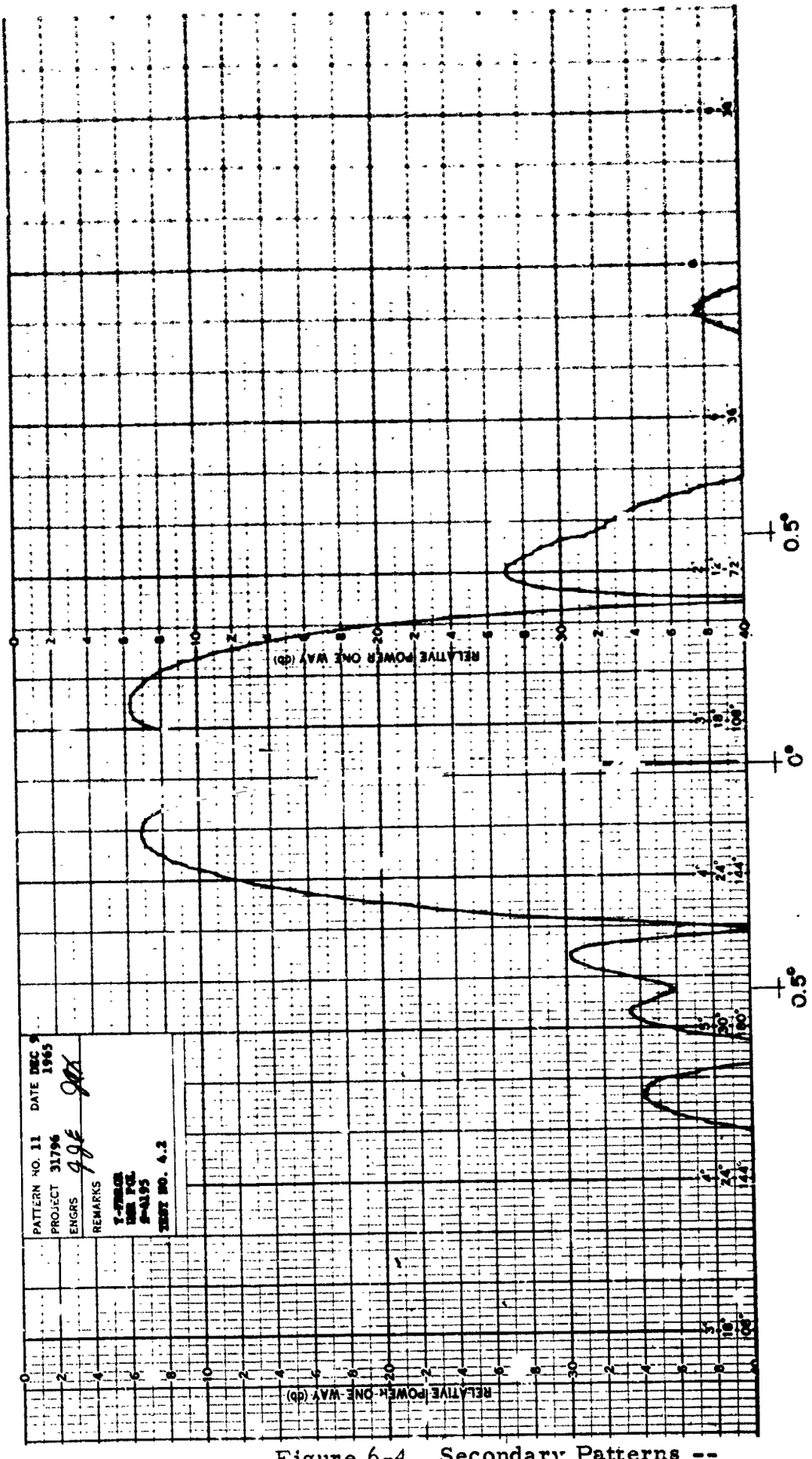

Figure 6-4. Secondary Patterns -- X & Y Error at 4195 Mc

Section 5.1 presents [illegible] pattern null depths were better than 35 db for both X and Y. During tests at Roseman, Early Bird satellite was tracked and attempts made to verify that the X-null is deeper than 35 db by plotting on the beacon Early Bird. It was shown that the null was at least 20 db deep, at which point the signal dropped out. Aircraft tracks showed the X and Y tracking to be of equal quality with the standard tracking deviations from optical boresight being 0.[illegible]^{0} for X and 0.024^{0} for Y. These numbers are for fitted data with mean deviation from optical boresight set to zero.

Because of the Roseman pattern range characteristics, difficulties were encountered in boresighting the Cassegrain feed system. Pattern and gain measurements were made with the subreflector mechanically centered and aligned on the geometric major axis of the antenna. The subreflector was adjusted axially along the major axis to the focal plane for optimized Y-cut patterns. The Y-null occurred within 0.003 degree of optical boresight. The X-null was 0.074 degree from boresight. However, the aircraft tracks showed the X-boresight to be only 0.002 degrees from optical with Y showing the large mean deviation of 0.058 degrees. The data indicates that the Y deviation is only about 0.020 degrees when the plane was at 30^{0} elevation in the vicinity of the collimation tower. This is the lowest elevation angle flown. This information indicates that precise boresighting will have to be done by a series of subreflector adjustments and aircraft tracks because of the erroneous information obtained by using the Bald Knob collimation tower.

Optimum focusing was obtained with the subreflector vertex 210.8 inches from the weather window surface at the top of the cone. From the Cassegrain geometry information contained in Figure 4-2 the tracking array and horn phase centers would occur 1.9 inches below this surface.

The measured difference in gain between the communications horn sum channel and the peak of the error channels was 10.8 db. The factors involved in this figure are estimated as follows: 3 db loss in the circularly polarized horns of the tracking array; 3 db loss to spillover beyond the subreflector as a result of the high sidelobes on the primary pattern; 2.5 db gain loss for the aperture used in the difference mode;[6] 1.8 db loss in the power dividers, 90° hybrid and comparator cables. These estimates account for 10.3 db gain difference. The spillover and difference mode estimated losses are probably low and could account for the other 0.5 db.

The aperture, i.e. the circular array with the blank area in the center for the communications horn, results in high sidelobes far from boresight which become large spillover contributions.

6.3.2 Tracking Accuracy - An estimate of tracking accuracy can be made by considering the errors resulting from receiver noise, phase errors, and comparator amplitude unbalance. The error channel slope is involved in quantitative consideration of all these errors. This slope is defined as the rate of change of the received error signal normalized to the sum channel output at boresight. Thus the units are volts per volt per degree. The measured Y-error channel slope at 4105 Mc was 3.2 volts/volt/degree. Only the measured Y-error data will be used for this analysis because the ground reflections and phase errors in the X-patterns result in an erroneous calculated slope of 1.4 volts/volt/degree.

6.3.2.1 Receiver Noise - Rms tracking error can be related to slope, signal level, and noise level by the formula

$$\Delta\theta = \frac{1}{K}\sqrt{\frac{N}{S}}$$

[6] R. Kinsey, "Monopulse Difference Slope and Gain Standards," IRE Transactions on Antennas and Propagation, Vol. AP-10, No. 3, May 1962, pp. 343, 344.

where

$\Delta\theta$ is the standard deviation of a large number of measurements of target position, and also the angle by which the antenna must be pointed away from the target for unity signal-to-noise ratio in the error channel.

K is error channel slope (3.2 volts/volt/degree)

S/N is signal-to-noise ratio

For a 40 db signal-to-noise ratio, typical for this application, $\Delta\theta = 0.0031$ degrees. This is approximately 1.55% of the sum channel beamwidth.

6.3.2.2 Phase Errors - Simultaneous pre-comparator and post-comparator phase errors are required to produce a boresight shift. An approximate formula for this boresight shift is

$$\Delta\theta = \frac{1}{2K} (\sin \phi) (\tan \phi_2)$$

where

ϕ_1 = pre-comparator phase unbalance

ϕ_2 = post-comparator phase unbalance

For this system, the cables were tested and trimmed using the Rantec phase measurement equipment which has the accuracy of $\pm 0.25^\circ$. The cables for the comparator network were within 6° of being identical. This 6° pre-comparator together with 10° post-comparator gives

$\Delta\theta = 0.0029^\circ$ or 1.4% of the beamwidth

6.3.2.3 Comparator Amplitude Unbalance - Boresight is related to amplitude unbalance by the formula

$$\Delta\theta = \frac{1}{K} \left(\frac{1-\alpha}{1+\alpha} \right)$$

where

$20 \log \alpha$ = unbalance in db

Amplitude unbalance can be estimated from the component test data or calculated from the actually measured error channel null depths for the four-horn system used here.

Component tests of the 2 to 1 power splitter and 90° hybrid showed 0.1 db unbalance each. The 4 to 1 power splitter and four horns in each quadrant can be considered as an entity since the amplitude unbalance of 0.5 db among the four horns in a quadrant has negligible effect on the main beam radiated from that quadrant. As mentioned previously, diagonal quadrants are compared so that the axial ratio of the horns themselves is not a contributing factor to unbalance. Thus, the component data would indicate about 0.2 db total unbalance.

Unbalances are related to null depth by the formula

$$\text{null depth} = 20 \log \frac{1+\alpha}{1-\alpha}$$

where unbalance in db = $20 \log \alpha$

For a 30 db null, the specified minimum, the unbalance is 0.51 db. Actually, the unbalance was kept below this value and null depths of 34 db or greater were achieved which corresponds to unbalances of 0.35 db or less. The null depths were dependent upon polarization with 40 db nulls (0.175 db unbalance) often measured. It is felt that this polarization dependence is caused by changes in aperture blockage and ground reflections.

Applying the formula for boresight error results in

$\Delta\theta$	% of beamwidth	Unbalance
0.0032°	1.6%	0.175 db
0.0036°	1.8%	0.2
0.0063°	3.1%	0.35

To summarize, the rms tracking error caused by receive noise is 0.0031 degrees. The maximum combined boresight shifts as calculated can be 0.0092 degrees. There can also be boresight shift with polarization which is specified at ±0.006 degrees and measured to be 0.004 degrees for the Y-axis. Note that the boresight shifts represent an error between electrical and mechanical axes of the antenna and represent negligible error in the tracking function of keeping the sum channel beam on target. The same will be true of mechanical sources of boresight shift.

6.4 Polarization Tracking - The polarization sensing and rotation experiment performed at Rosman between the 85-foot antenna and Bald Knob collimation tower showed polarization tracking errors between the two antennas of almost 5 degrees. 180 degree rotation of the collimation tower antenna caused about 4 degrees shift in the null received at the 85-foot antenna. Furthermore, the two nulls were 26 and 45 db at one time of day and both were 35 db at another time. These effects are believed to be caused by changes in the collimation tower antenna with 180^{o} rotation because of the tripod support structure as well as changes in the antenna range reflection characteristics caused by temperature and moisture characteristics.

Initial polarization tracking experiments at Rantec resulted in similar errors, i.e. widely different null depths with rotation and tracking errors of several degrees. These experiments were performed on the 365 foot pattern range.

Reduction of the distance between the communications horn and the calibrated horn to 7-feet and covering of all antenna range towers and stands with hairflex to suppress reflections improved the tracking accuracy so that the error was reduced to ±0.27 degree. The null depths were measured and found to be between 39.5 db and 44.8 db for all rotation angles.

Polarization calibration of the 6-foot diameter collimation tower antenna was done on a 30-foot range with the same precautions described above to suppress reflections. Tracking was within ±0.6 degree with null depths ranging between 29.2 db and 33.1 db.

In an effort to eliminate the Rosman antenna range reflection characteristics an experiment was performed with a horn mounted at the vertex of the hyperboloid and beamed at the top of the cone. No provisions were made for precise rotation of this test horn. However, rotation of the communications feed horn produced identical nulls at the 180° points and the nulls were within 0.08° of 180° as read out on the polarization rotation indicator dial.

It is understood that a similar but highly refined polarization calibration system is being built for installation on the 85-foot antenna. Rotation of the horn on the subreflector will be remotely controlled and its position determined from a remote readout. A receiver is being provided with the provisions for amplitude and phase adjustments to cancel unwanted signals as discussed in Section 5.7 of this report.

6.5 Noise Temperature - Preliminary noise temperature measurements were made by Goddard Space Flight Center on the Cassegrain Feed System in the 85-foot antenna. These measurements were made at the Maser input flange using the radiometer developed by Philco Western Development Labs. The technique was not highly refined in that the antenna temperature was compared to room temperature and dry-ice cooled loads. Accuracy could be enhanced by use of nitrogen or helium-cooled loads for the reference temperature. The measured noise temperature was 23 - 25°K with the antenna at zenith.

SECTION VII

CONCLUSIONS

The equipment developed under Goddard Space Flight Center Contract No. NAS 5-3564 and discussed herein has satisfactorily met the required specifications. The design approach has resulted in a reliable feed system with inherently low repair rates. The waveguide components will require no maintenance with the semi-rigid cables and electronics equipment requiring a minimum of periodic servicing and replacement of parts.

Rantec No. 31796-ER1 15 June 1966

Final Engineering Report
for
Polarization Alignment Receiver

Prepared for

NASA

Goddard Space Flight Center

Greenbelt, Maryland

Rantec Project No. 31796 Government Contract No. NAS 5-3564

Prepared by: D. G. Carson
D. G. Carson

Approved by: C W Smith

RANTEC CORPORATION
CALABASAS, CALIFORNIA

1.0 SCOPE

This report describes a solid state, dual channel, phase lock receiver. It is intended for polarization alignment of a Cassegrain Feed System for an 85-foot Antenna as per Specification No. GSFC-TRS-ANT-23, Revision No. 1, dated 25 March 1963. The design criteria, performance specifications, and test procedures and results are given.

2.0 GENERAL

A block diagram of the polarization alignment system is shown in Figure 1 with the receiver connected to the Monopulse Converter, low noise RF circuitry, and dual mode transducer. The following system boundary conditions were specified:

Minimum input signal strength:	-102 dbm
Polarization error measurement capability:	$\pm 0.1^{\circ}$
MASER & TWT amplifier gain:	50 db nom.
MASER noise temperature:	10°K max.
Antenna noise temperature:	30°K max.
Monopulse converter noise figure:	8 db max.
Monopulse converter gain: (mixer: -6 db; preamp: +30 db)	24 db min.
Cable loss (converter to receiver)	3 db nom.
Tracking receiver reference channel output required	

Assumed System Boundary Conditions are as follows:

System dynamic range: (max. input signal: -42 dbm)	60 db
Maximum monopulse converter input signal:	-10 dbm
Linear polarization error indication: (0.1 to 10 degrees)	40 db

2.1 Dual Mode Transducer

The dual mode transducer which generates the polarization alignment error signal has a null voltage output proportional to the sine and a reference output voltage proportional to the cosine of the polarization error angle. The null output voltage has a 180 degree relative phase relationship on each side of the null. For a 0.1 degree polarization error, therefore, the normalized null output voltage is:

$$\sin 0.1 \text{ degree} = \frac{0.1 \text{ deg}}{57.3 \text{ deg/rad}} = 0.00174$$

and the minimum relative reference/null signal strength is:

$$20 \log \frac{1}{0.00174} = 55.2 \text{ db}$$

2.2 Signal Levels

Full system capability was specified as required with a beacon input signal to the dual mode transducer of -92 dbm. A 10 db safety margin results in a threshold signal of -102 dbm.

The polarization error signal enters the converter prior to any amplification. It will be at a level of -157 dbm at the dual mode transducer for a 0.1 degree polarization error. The input to the monopulse converter will be at the -160 dbm level after going through the phase compensating rotary joint. The 55 db channel-to-channel isolation within the converter requires that the sum signal enter the converter at a level of -105 dbm or less to prevent fill-in of the polarization error null. Hence, the sum signal must enter the converter 3 db below its level at the dual mode transducer. The 3 db drop is experienced in the phase compensating rotary joint. Any sum signal gain in the Maser and TWT must be removed prior to the converter. This is accomplished by 30 db coupling to the signal from the Maser/TWT output and an additional attenuator. The attenuator value was determined during system checkout to be 27 db.

Equalization of the channel gains prior to the receiver permits operation of the polarization alignment system with the Maser and TWT removed from the reference channel. In addition, testing of the system at any point prior to the receiver can be accomplished by synthesizing the dual mode transducer operation with true relative reference-null channel signal strengths.

Since a 40 db linear polarization error output is required for 0.1 to 10 degrees (null channel -55 db to -15 db relative to reference channel), the relative null channel gain can be increased by 15 db, increasing the error output level while maintaining the required error signal within the amplifier linear range. However, a 15 db attenuator in the reference channel input is the most desirable method of increasing the error channel relative gain. It limits the maximum differential channel-to-channel signal strength to 40 db (eases channel-to-channel isolation requirement) as close to the receiver input as possible and permits identical following receiver channels for minimum differential gain and phase shift versus AGC, tuning, etc. Removal of the 15 db attenuator will increase the reference channel sensitivity from -105 to -120 dbm and decrease the polarization error indication by a factor of 5.5 (minimum indication increased from 0.1 to 0.55 degrees).

On the following page is a tabulation of the signal conditions throughout the system.

Threshold	Null Channel 0.1 degree	Null Channel 10 degree	Ref. Channel
Dual Mode Transducer Output	-157 dbm	-117 dbm	-102 dbm
Monopulse Converter Input	-160 dbm	-120 dbm	-105 dbm
Preamplifier Input	-166 dbm	-126 dbm	-111 dbm
Monopulse Converter Output	-136 dbm	-96 dbm	-78 dbm
Receiver Input	-139 dbm	-99 dbm	-84 dbm
Receiver Mixer Input	-139 dbm	-99 dbm	-99 dbm
Receiver IF Input	-145 dbm	-105 dbm	-105 dbm
Receiver IF Output Signal (70 ohms)	0.0025vRMS	0.25vRMS	0.25vRMS
Receiver IF Output Noise due to System Input	0.100vRMS	0.100vRMS	0.078vRMS
Receiver IF Output Noise due to Receiver only	0.0252vRMS	0.252vRMS	0.0252vRMS
Maximum Signal			
Dual Mode Transducer Output	-97 dbm	-57 dbm	-42 dbm
Monopulse Converter Input	-100 dbm	-60 dbm	-45 dbm
Receiver Input	-79 dbm	-39 dbm	-24 dbm
Receiver Mixer Input	-79 dbm	-39 dbm	-39 dbm
Receiver IF Signal Output (70 ohms)	0.0025vRMS	0.25vRMS	0.35vRMS

Miscellaneous

2nd Mixer Input Level	1.0 mw
3rd Mixer Input Level (from 50 ohm source)	0.15vRMS
Synchronous Detector Reference Level	0.23vRMS

2.3 Receiver Tuning

The receiver is either fixed tuned to 136 Mc by crystal control or tunable ±0.250 by a VFO; selection is by front panel switch. The crystal control permits operation and testing of the receiver in its most stable form when a variable signal source is available or when the input frequency is accurately known (crystal replacement can provide for frequency change). The range of the VFO which tunes the receiver to 136 ±0.250 Mc is the minimum permitted by the specification. This minimizes the vernier tuning range and facilitates phase lock loop signal acquisition. The vernier tuning has a 5:1 gear reducer.

2.4 Phase Lock Loop

The phase lock loop bandwidth is nominally 300 c/s, achieved in a second order loop. This permits receiver operation with signal sources which contain large amounts of 60 c/s and harmonic phase modulations (ordinary signal generators). Reduction of this bandwidth is not necessary for sensitivity reasons since the threshold input signal-to-noise ratio to the phase detector is 20 db.

The impedance of the loop filter was made as low as possible, using the largest practical capacitor, permitting future reduction of the loop bandwidth if desired by changing two resistor values.

The VCXO has a ±0.06% tuning range with the ±10 VDC control voltage available from the phase detector. This provides a ±24 kc automatic frequency tracking range since it generates the 40 Mc second L.O. A ±10% (2.4 kc) automatic acquisition range was demonstrated.

2.5 Polarization Error Indication

While the coherent polarization error amplitude detector output is linear over 40 db (error channel -55 db to -15 db relative to reference channel), increased meter deflection is required to provide satisfactory indications at the smallest required polarization errors. An expanded

null meter has been used and an increased sensitivity position incorporated by increasing the gain of the amplitude detector by 26 db. The following approximate meter indications result:

	Sensitivity	
Condition	Normal	Increased
Full scale	Saturated (45 degrees)	2 degrees
3/4 scale	20 degrees	1 degree
1/10 scale	2 degrees	0.1 degree

The two 90 degree phase adjustments in the reference outputs to the phase and amplitude detectors are used to maximize the polarization error indication. This adjustment should be made with an indicated error of less than 10 degrees. Since the line lengths are not the same between the dual mode transducer and the receiver (MASER and TWT in reference channel), this phase adjustment must be made when the signal frequency is changed.

2.6 Receiver Specifications

The performance specification for the receiver portion of the polarization alignment system is as follows:

Frequency Input	136 ±0.25 Mc (min)
Reference Channel	
Threshold	-84 dbm (nom)
Dynamic Range	55 db (min)
Null Channel	
Min. Rel. Signal Strength	-55 db
Output at -55 db rel.	±100 mv (min)
Dynamic Range	40 db (min)
Automatic Frequency Tracking Range	±24 kc (nom)
Automatic Frequency Acquisition Range	±2 kc (nom)
Isolation between Channels	70 db (min)
Phase Stability	±3 degrees (nom)
Amplitude Stability	±1.5 db (nom)
Phase Lock Loop Bandwidth	300 c/s (nom)
2nd IF Bandwidth	12.5 kc (nom)
AGC Bandwidth	35 c/s (nom)

3.0 RECEIVER TEST AND EVALUATION

Tests were performed, as described in the following paragraphs, to determine actual receiver performance.

3.1 AGC Control Characteristic

The AGC control characteristic is shown in Figure 3 after proper adjustment. The test setup of Figure 2 was used to adjust for proper operation and obtain the data. The power split system insertion loss was measured at 23 db; signal level plotted is actual receiver input signal strength. Adjustment procedure requires:

1. Reduce IF gain from maximum (manual adjustment) of highest gain channel until 0.2v RMS is obtained out of both IF amplifiers with the input frequency (136 Mc) tuned for maximum output and at required input level (approximately -87 dbm).
2. Adjust AGC threshold to start AGC voltage increase at 0.25v RMS reference IF output.
3. Adjust AGC gain for +10VDC AGC at 0.35v RMS reference IF output.
4. Reduce from maximum either null or reference AGC level to obtain flattest null IF output over full input signal level range (reference loop phase locked).

The curves show less than ±1.0 db error channel output (polarization error indication) over a 60 db input signal level range. A 4:1 AGC control slope change gives a measured AGC bandwidth of approximately 100 c's at threshold to 25 c's at maximum signal input.

3.2 Polarization Error Indication and Sensitivity

Test Setup No. 2 shown in Figure 4 was used to obtain polarization error indication and sensitivity data. The power splitting system which includes pads R1 and R2 provides equal isolated outputs with a measured insertion loss of 23 db. Variable attenuator R3 is used to simulate

polarization error by adjusting relative error-reference channel signal strength. Peaking of the error indication with the receiver phase shifters completes the simulation. The preamplifiers in the monopulse converter are included to assure that their noise contributions do not degrade the system performance. The R4 and R5 attenuators simulate the 500-foot cable loss between the monopulse converter and the Instrumentation Building where the receiver is located. The R6-6 db maximum variable attenuator equalizes the channel gains (as shown, Δ Channel had the highest gain). In actual operation, as shown in Figure 1, an additional 27 db nominal attenuator is required in the receiver reference channel to equalize the channel gains by removing the excess MASER-TWT gain.

Figure 5 shows the output indication as a function of simulated polarization error. Normal sensitivity full scale indication occurs for polarization errors in excess of 45 degrees (saturated output). The 1/10 scale indication is considered the minimum satisfactory indication. Two (2) degrees is the full scale increased sensitivity indication and the 1/10 scale normal sensitivity indication.

Figures 6 and 7 (increased and normal sensitivity, respectively) show the indication for various simulated polarization errors as a function of signal strength. The signal strength indicated is the equivalent system reference channel input calculated as follows:

	At Threshold
Signal generator level	-85 dbm
Power split loss	-23 db
	-108 dbm
Preamp 3 db measured mismatch loss (50 ohm source rather than 200 ohm mixer impedance)	-3 db
	-111 dbm
6 db mixer conversion loss	+6 db
	-105 dbm
Rotary joint loss	+3 db
	-102 dbm

The ability to indicate polarization error below the system design threshold is of interest. The phase lock loop maintained lock-down to -130 dbm. Below this, it is difficult to determine if the loop is locked since the error indication and dynamic phase error beat note are small. The 300 c/s phase lock loop bandwidth at threshold provides a VCXO control S/N ratio of approximately 35 db. This is maintained below threshold due to loop gain reduction of loop bandwidth; a corresponding reduction in loop frequency tracking range results, however.

As shown in Figure 6, it is difficult to indicate polarization error outputs less than 0.1 VDC. This is due to noise. Since the error output at threshold for 0.1 degree polarization error (-55 db relative, and -160 dbm absolute error channel signal strength) is 0.10 VDC, the noise voltage output is 0.050v RMS for a 1.0 cycle meter bandwidth and a 8 db system noise figure (174 - 8 = -166 dbm noise power input). This limitation does not appear in Figure 7 since the insertion of the 26 db attenuator to reduce sensitivity reduces the noise output correspondingly.

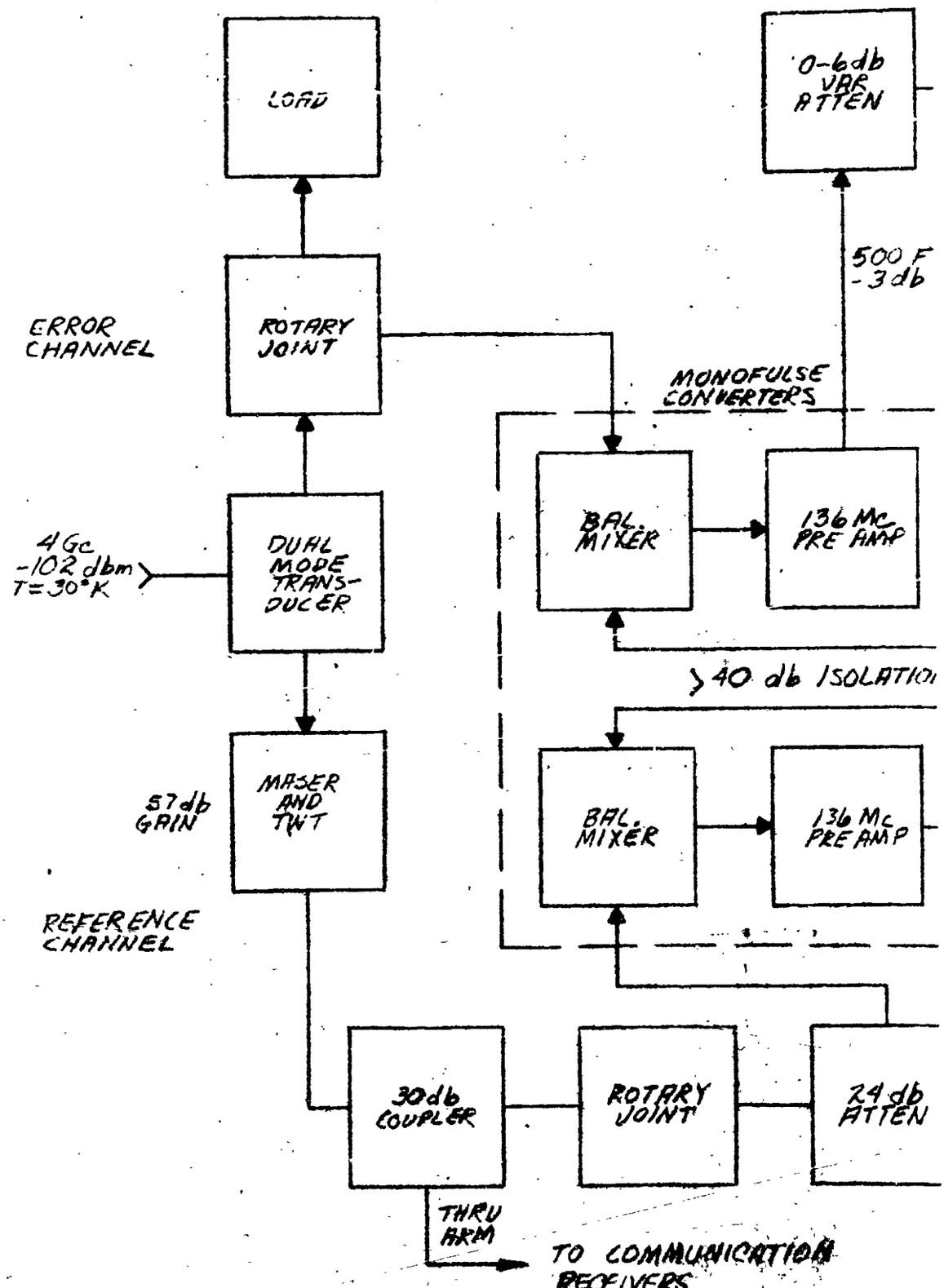
LOAD
0-6db VAR ATTEN
500 F -3db
ERROR CHANNEL
ROTARY JOINT
MONOFULSE CONVERTERS
BAL MIXER
136 Mc PRE AMP
4 Gc -102 dbm T=30°K
DUAL MODE TRANS-DUCER
> 40 db ISOLATION
MASER AND TWT
57 db GAIN
BAL MIXER
136 Mc PRE AMP
REFERENCE CHANNEL
30 db COUPLER
ROTARY JOINT
24 db ATTEN
THRU ARM
TO COMMUNICATION RECEIVERS

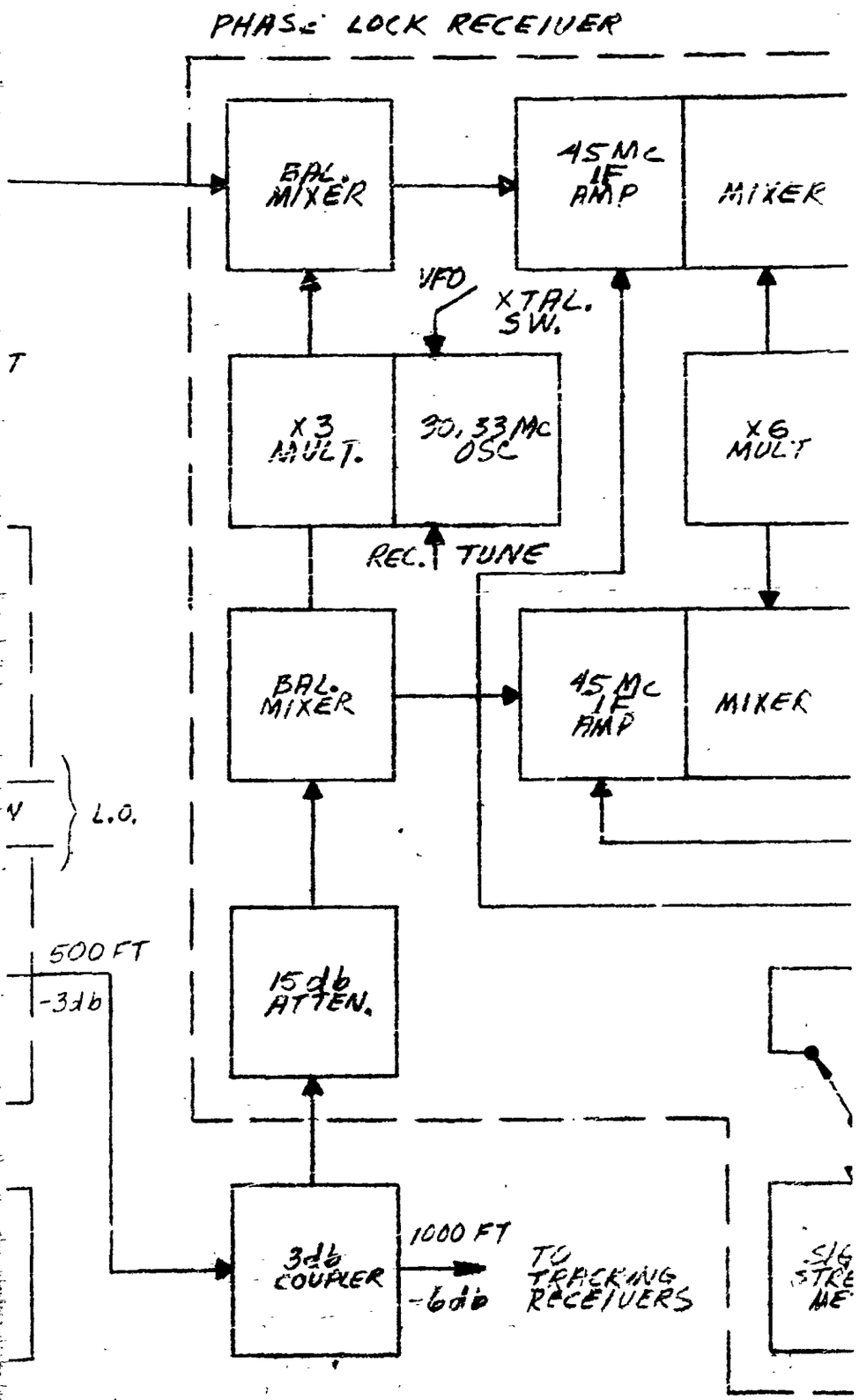
PHASE LOCK RECEIVER
BAL. MIXER
45 Mc IF AMP
MIXER
VFO
XTAL. SW.
T
X3 MULT.
30.33 Mc OSC
X6 MULT
REC. TUNE
BAL. MIXER
45 Mc IF AMP
MIXER
N
L.O.
500 FT
-3db
15 db ATTEN.
3db COUPLER
1000 FT
-6db
TO TRACKING RECEIVERS

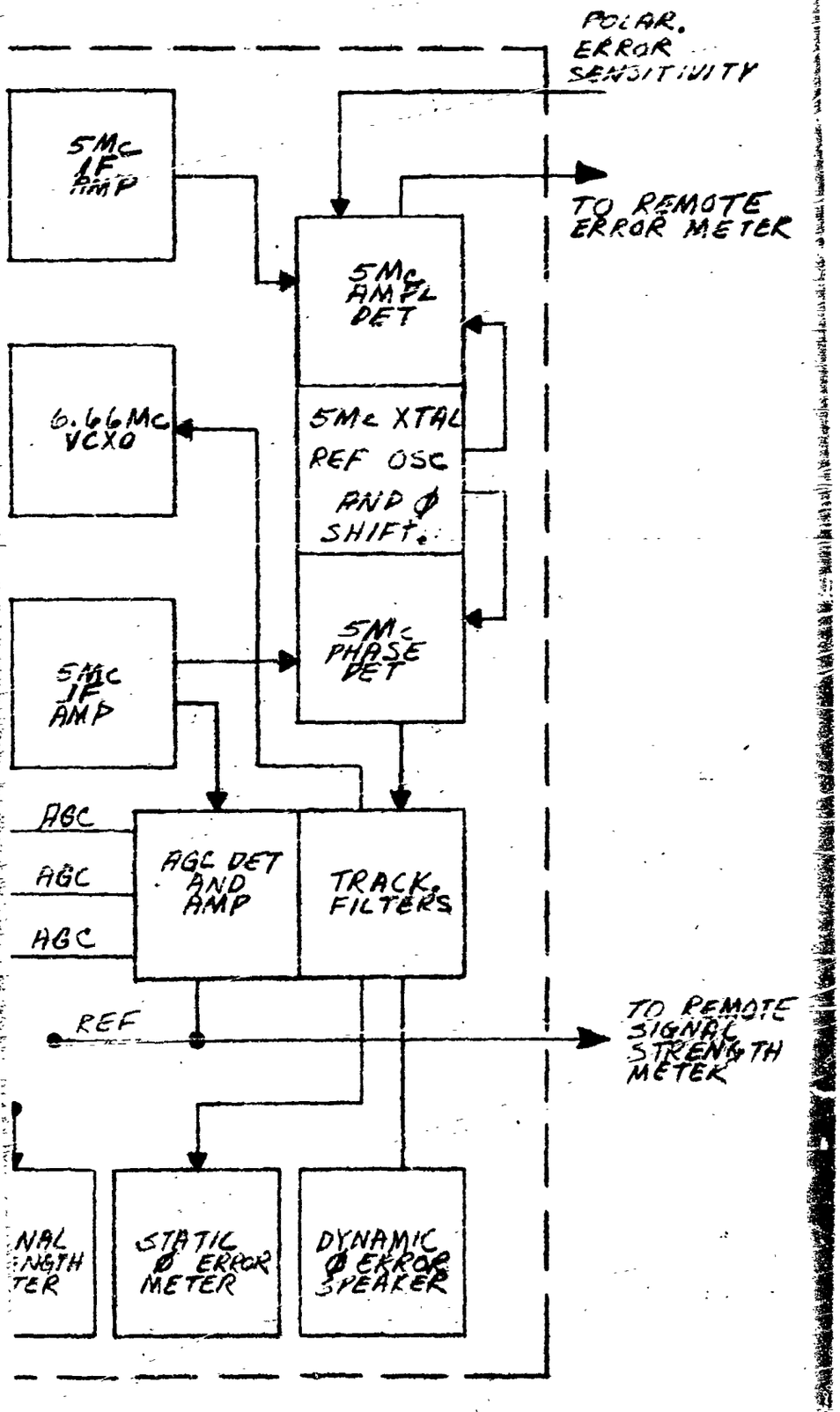

FIG 1-3

POLARIZATION ALIGNMENT SYSTEM BLOCK DIAGRAM

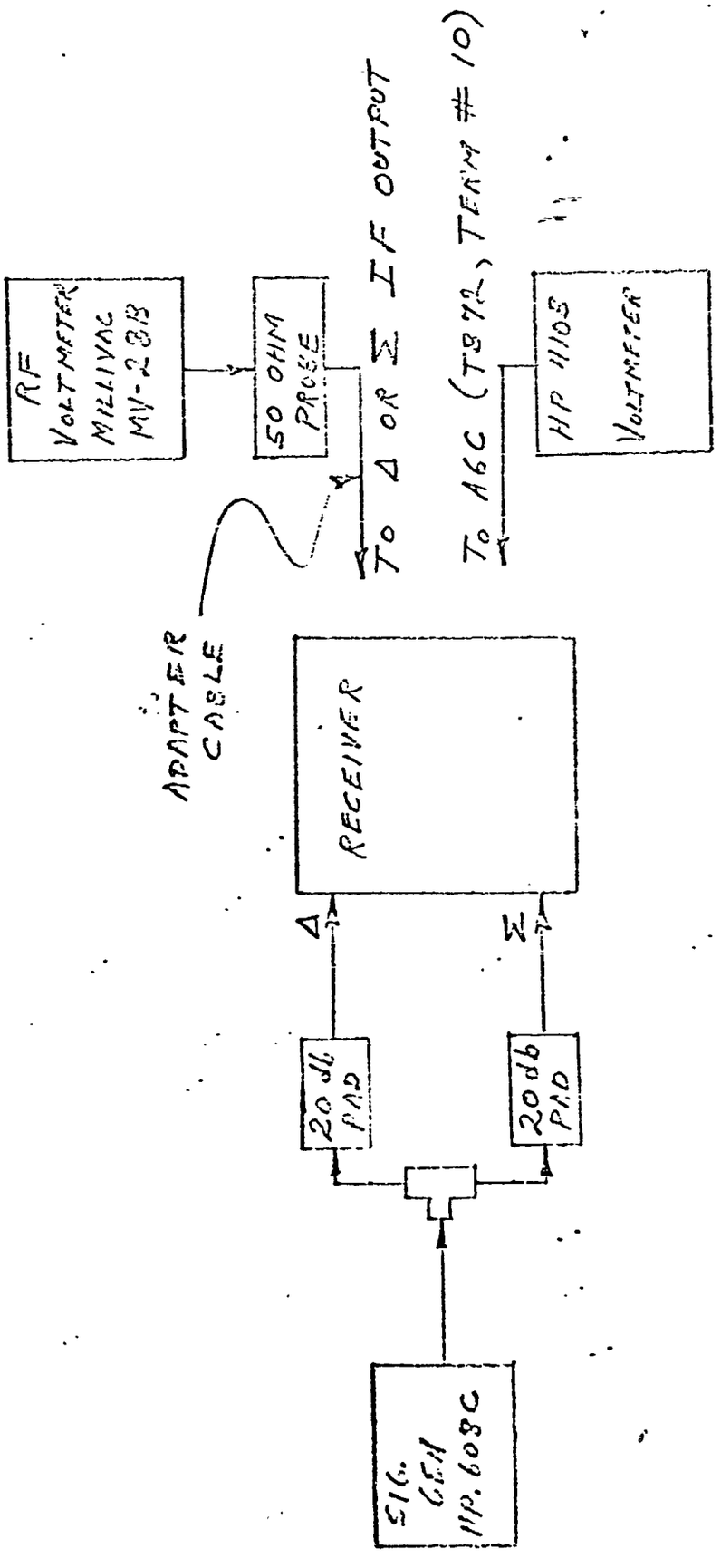

TEST SET UP #1

FIG. 2

Rantec No. 31796-FR1

15 June 1966

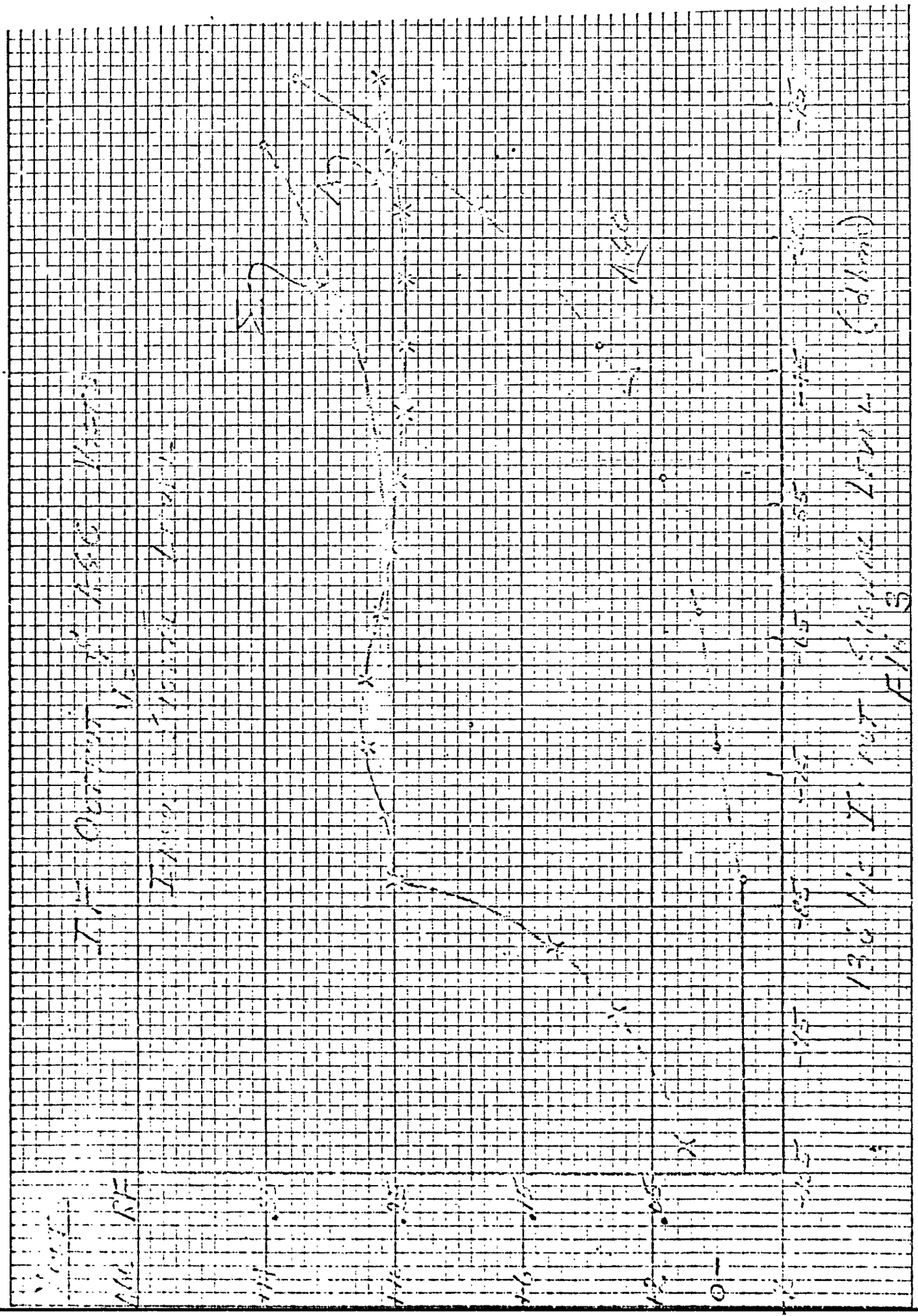

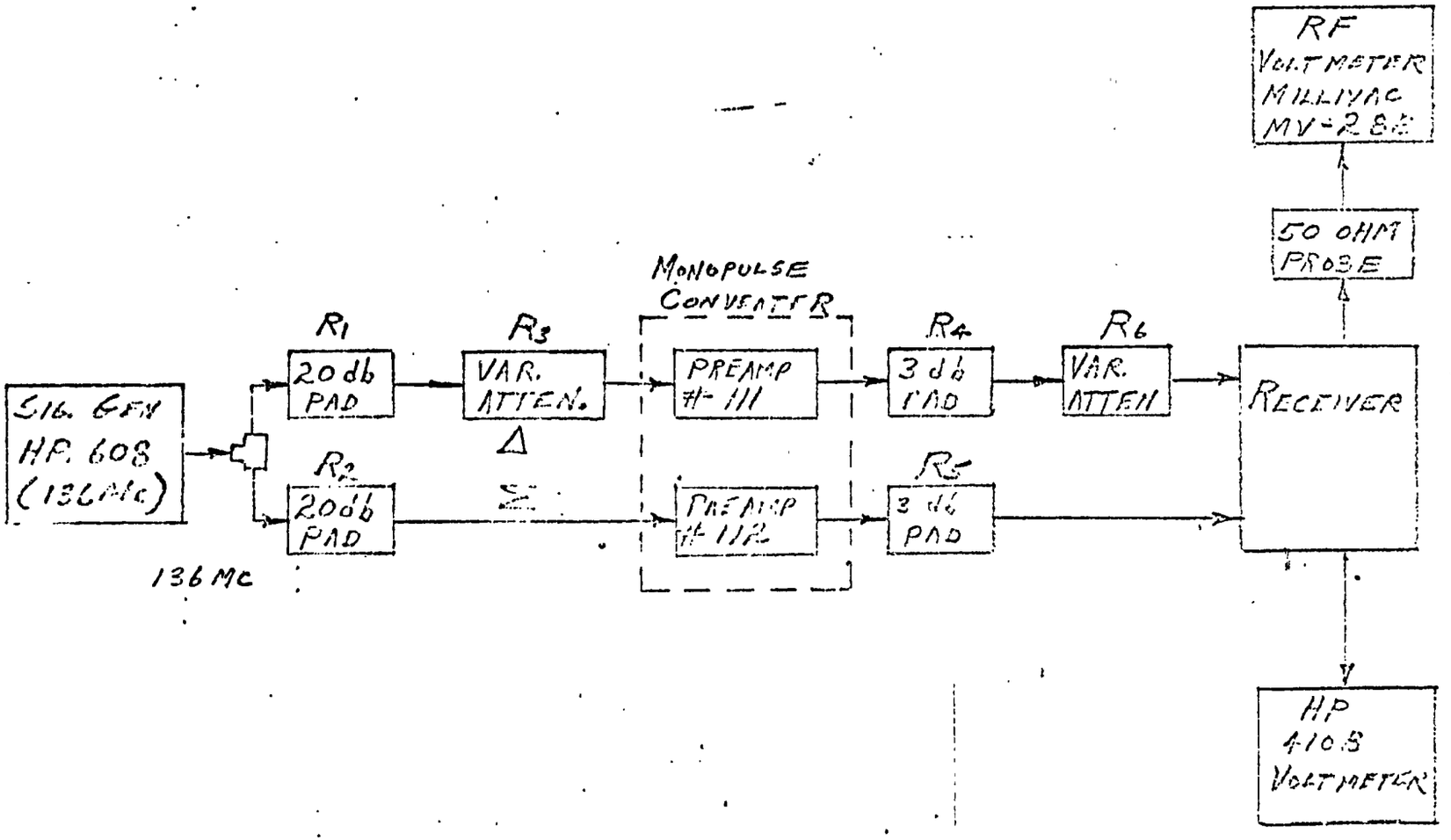

TEST SET UP #2

FIG 2

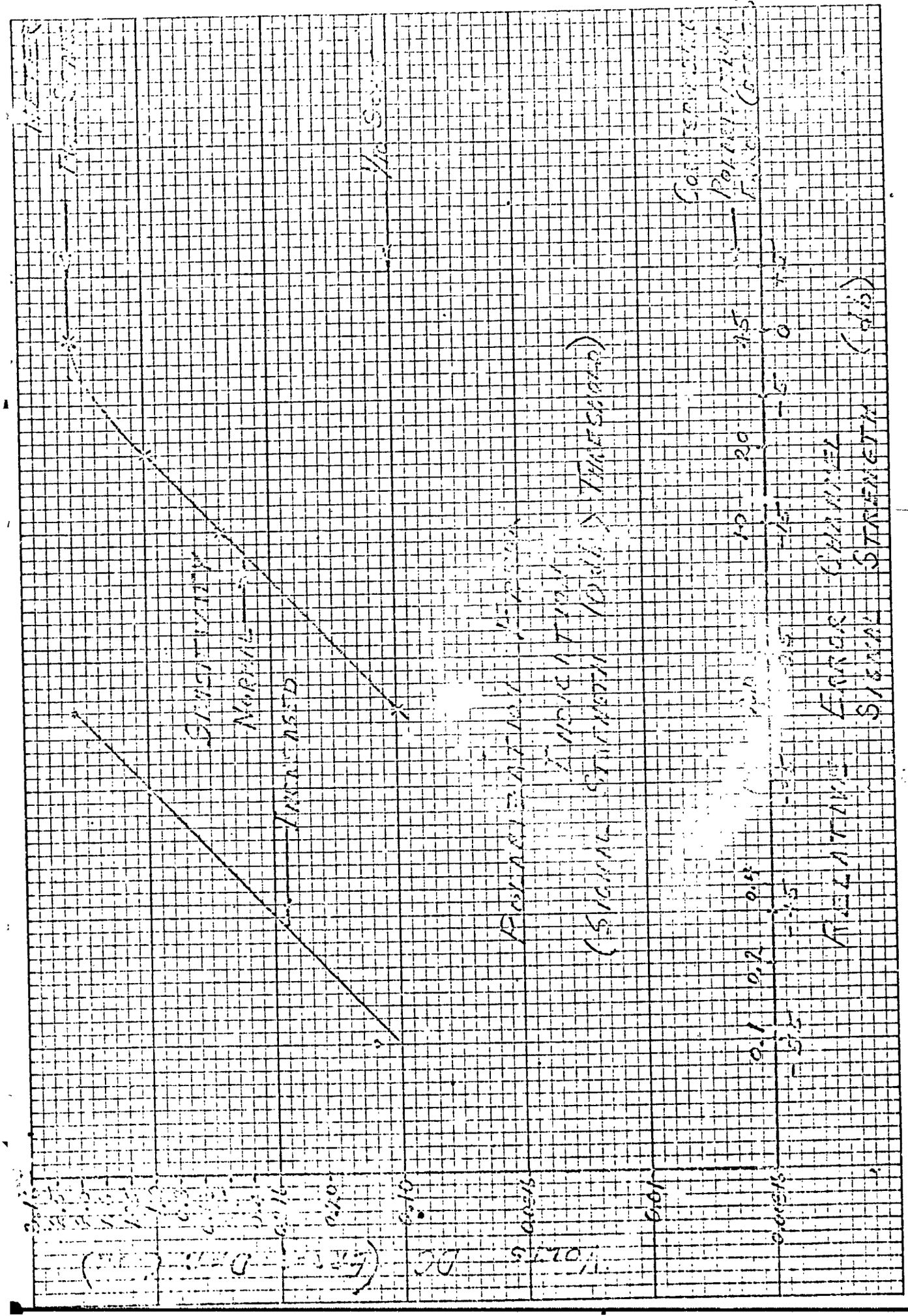

FIG. 5

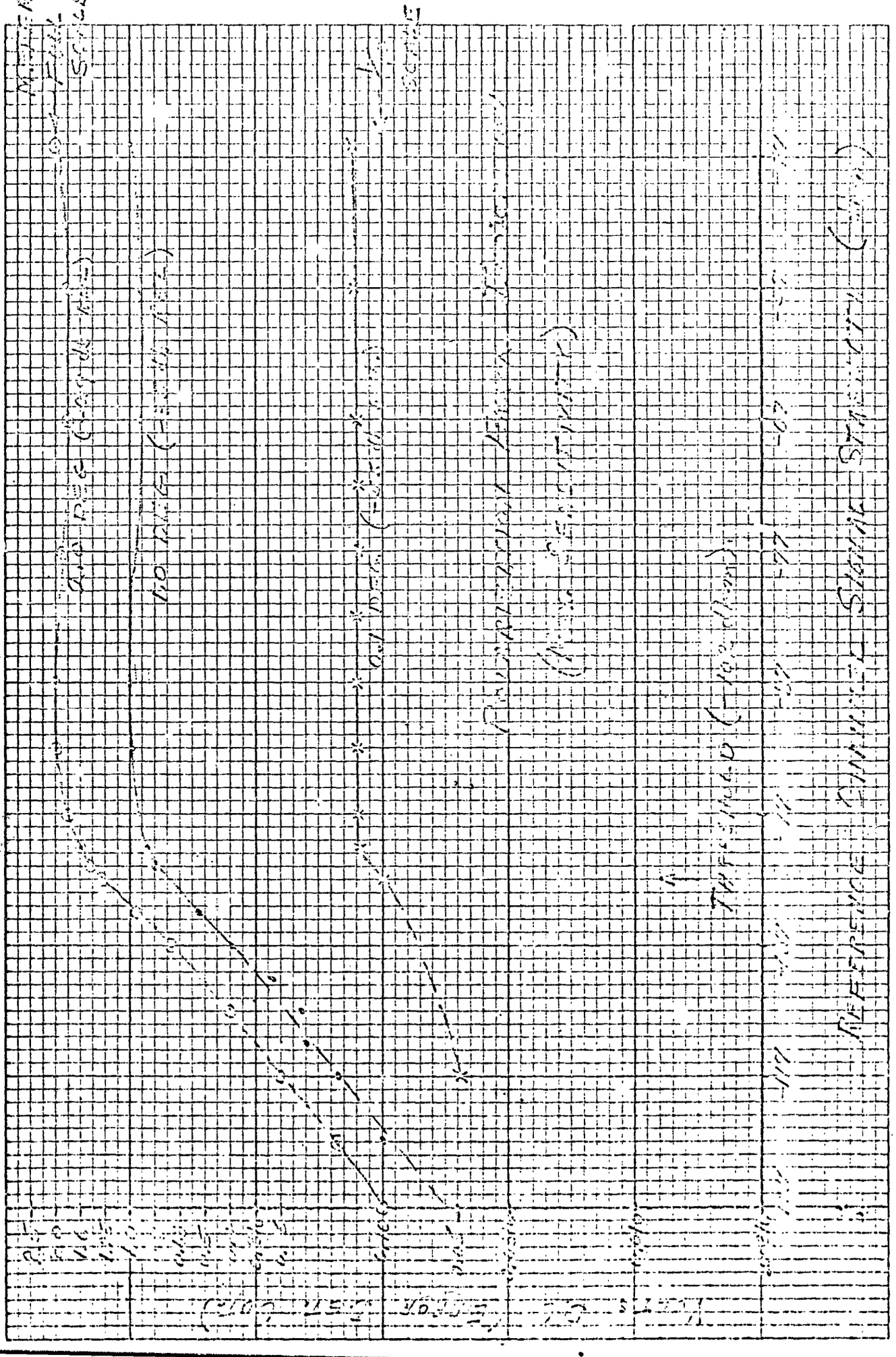

FIG. 6

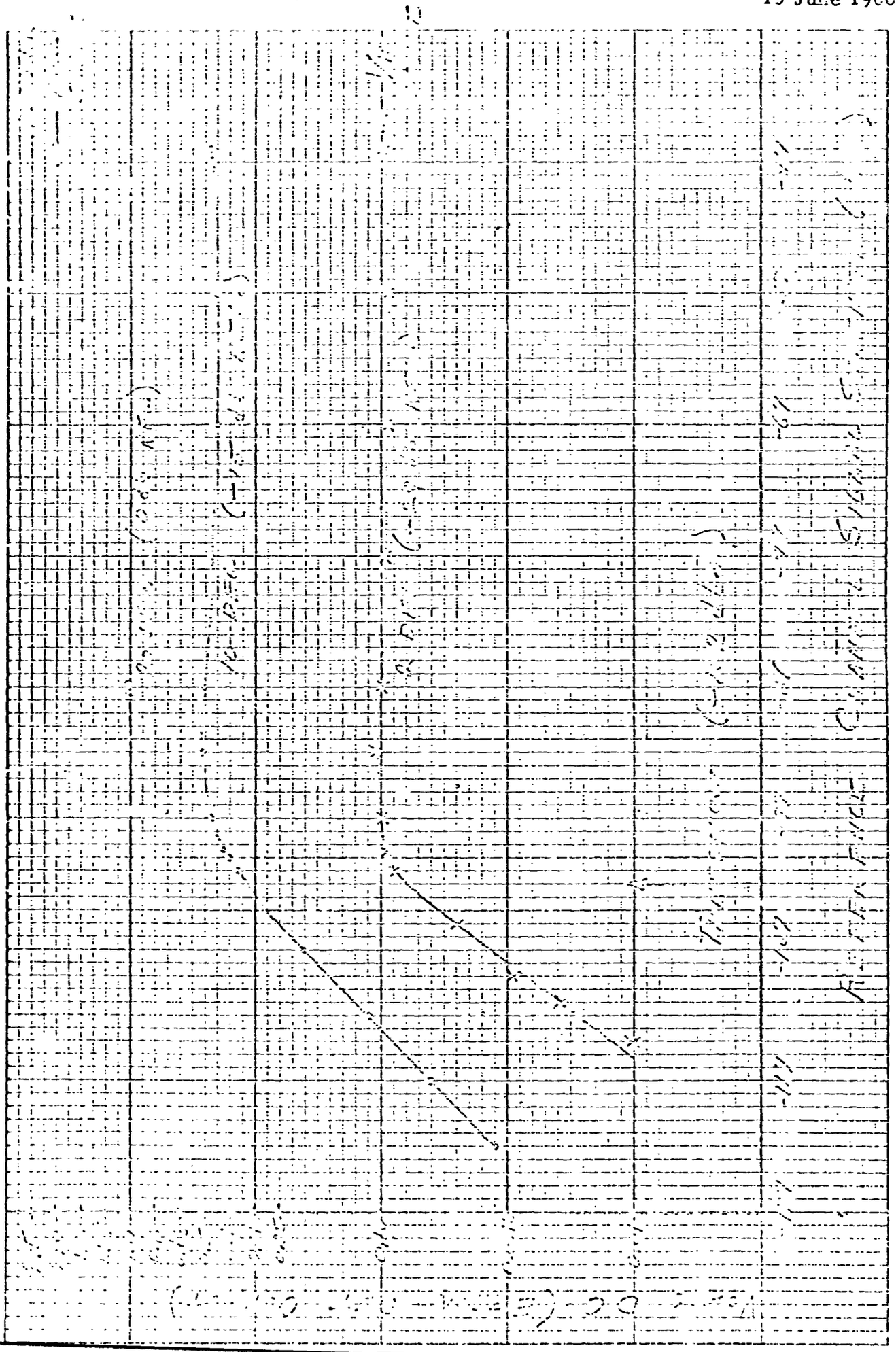

FIG. 2